ORIGINAL PAPER

Investigating the effects of climate change on future hydrological drought in mountainous basins using SWAT model based on CMIP5 model

Alireza Samavati[1] · Omid Babamiri[2] · Yousef Rezai[3] · Morteza Heidarimozaffar[3]

Abstract

Since climate change is a major challenge that affects the environment, especially the hydrological flow, this research has used the Soil and Water Assessment Tool (SWAT) to study the climate change effects on the runoff in Alvand mountain basin in Iran. The SWAT model calibration was done based on the SUFI-2 algorithm and the validation results for a 20-year prediction period (2020–2040) showed that the model had high accuracy in simulating the runoffs. CMIP5 models were used to predict the basin's temperature and rainfall (the best scenario was Miroc5) and the results showed that the basin's future climate conditions increase in temperature and decrease in rainfall were appropriate. According to Miroc5 (RCP8.5), the annual runoff in the mentioned period would decrease by 8.36% compared to the past. In a seasonal scale, the largest runoff reduction would be 75% in summer (under the Miroc5 (RCP4.5)), and in a monthly scale, it would be 79% in April increasing dramatically to reach 335% in September (under Miroc5 (RCP8.5)). The trend of the future runoff was investigated using the Mann–Kendall model and the Gresson estimation method. Results showed that there would be no significant trend in the mentioned period and the trend of the future drought intensity would be increasing under all studied scenarios.

Keywords Alvand mountain basin · Climate change · Hydrological drought index · Lars-wg6 · Mann–Kendall test · SWAT

1 Introduction

Climate change is a serious global challenge for the sustainability of water, energy and ecosystem processes and has very serious effects on the hydrological cycle. It is the result of the population growth, increased fossil fuel utilization, soil erosion deforestation and, hence, increased greenhouse gases (Li et al. 2016; Pachauri et al. 2014; Liu and Merwade 2018; Ashofteh et al. 2015a, b, 2017; Azadi et al. 2019; Liu et al. 2021). Studying the climate change parameters plays an important role in forecasting surface runoffs to identify and manage the water resources because climate change changes the rivers' hydrological regimes and, hence, the frequency and severity of floods making it necessary to study hydrological processes required for making environmental management decisions, allotting water resources, protecting rivers' ecosystems and restoring rivers (Chu et al. 2013; Sharifi et al. 2017; Chen et al. 2019). The main source of water demand is the runoff created by streams (Ercan et al. 2020). If water resources are not available there will be hydrological drought resulting in severe effects such as: (1) deteriorated water quality, (2) crop failure due to limited irrigation water, (3) reduced electricity generation, (4) disrupted river habitats and (5) limited recreational/economic/social activities (Mishra and Singh 2010).

Since this source does not sufficient, and the available fresh water resources are limited, water shortage will

✉ Alireza Samavati
  alirezasamavati1373@gmail.com

1 Civil Engineering, Faculty of Engineering, Bu-Ali Sina University, Hamedan, Iran

2 Department of Water Science Engineering, Bu-Ali Sina University, Hamedan, Iran

3 Department of Civil Engineering, GIS, Faculty of Engineering, Bu-Ali Sina University, Hamedan, Iran
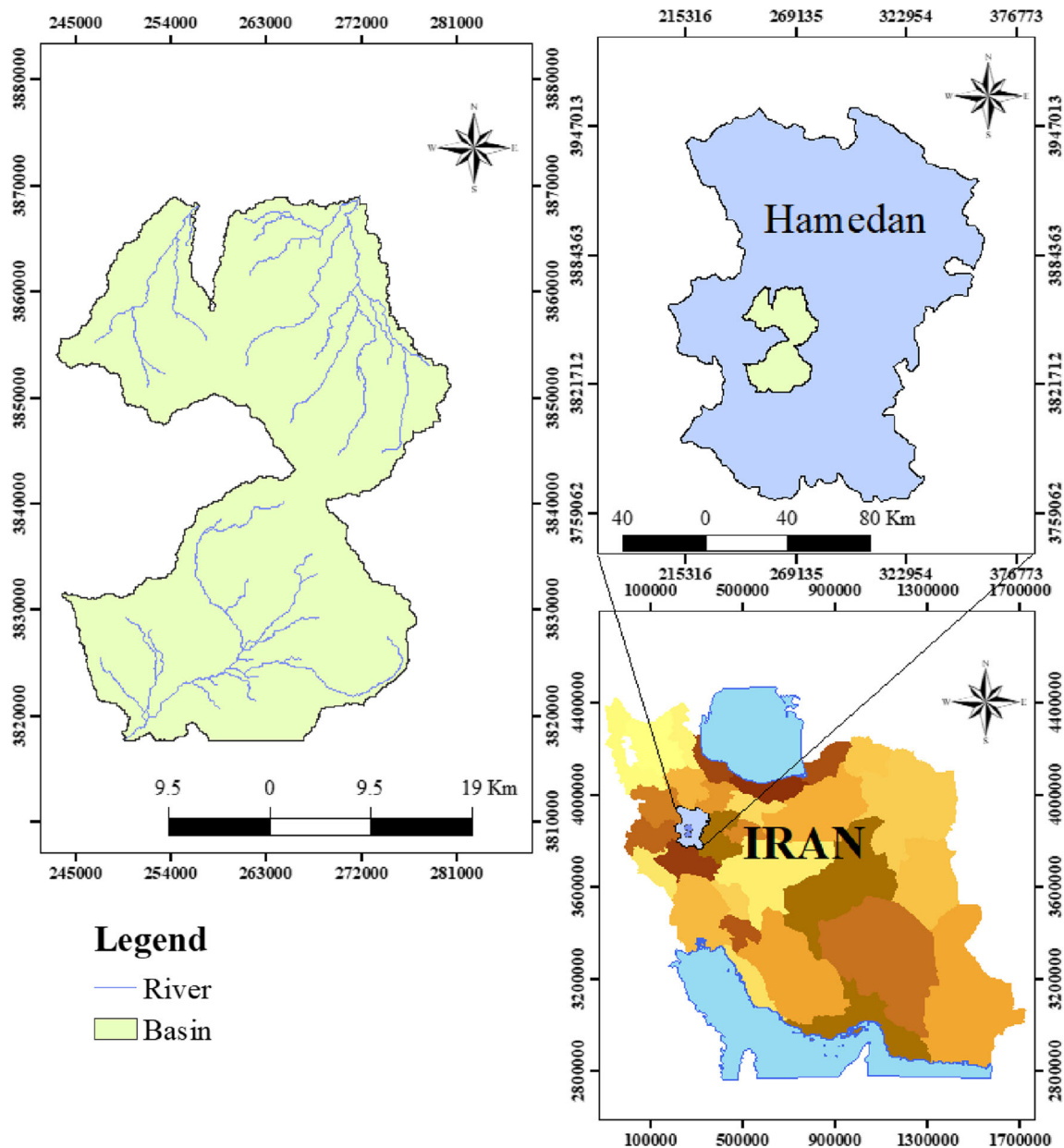
Fig. 1 The site Location of Alvand mountain basin, Iran

become a major future problem of the human societies. Therefore, more accurate prediction of the discharge and its variations during the year is a basic step in the planning and management of surface water resources (Shaigan et al. 2011). Naturally, since climate change affects runoffs, the hydrological drought index will also change in the future; in other words, the reduced runoff will increase the future drought periods and severity. Among researchers who have studied the drought index in previous periods, Babaeian et al. (2021) introduced a combination of adaptation pathway (AP) approaches that were used in conjunction with the SWAT model to evaluate the resilience of adaptation measures and design robust adaptation pathways

taking into account the future climate uncertainty in the Hablehroud River Basin. Salimi et al. (2021) studied the effects of the climate change on hydrological and meteorological droughts. They used Standardized Rainfall Index (SPI), SPEI and Standard Stream flow Index (SSI) in the Navrood and Lighvan watersheds in north of Iran and observed high correlation between hydrological and meteorological droughts. Also, they concluded that the climate change was the most effective factor in the occurrence of future droughts. Abdulai and Chung (2019) studied the meteorological and hydrological droughts caused by the climate change under the RCP4.5 scenario in the Cheongmicheon watershed in South Korea. Their

results referred to the occurrence of short-term severe or extreme droughts according to the standardized rainfall evapotranspiration index (SPEI) and streamflow drought index (SDI). Kamali et al. (2017) examined the climate change in the Karkheh river basin. They used the SWAT distribution hydrological model for runoff projection. They proposed the Drought Hazard Index (DHI), which is a combination of meteorological, hydrological, and agricultural droughts, and their results indicated the occurrence of drought based upon the DHI index. Studies conducted, so far, on the climate change effects on basins' runoffs include those of Xue et al. (2021), Kiprotich et al. (2021), Su et al. (2021), dos Santos et al. (2021), Chang and Su (2021), Lian et al. (2021), Li et al. (2021), Escanilla-Minchel et al. (2020) and Ridwansyah et al. (2020), just to mention a few.

Studying the effects of the climate change on runoff requires the latter to be simulated by hydrological models which are accurate tools necessary for the sustainable use of water resources and studying hydrological processes (Abbaspour et al. 2015). A comprehensive, accurate hydrological model available for studying the hydrological and biogeochemical effects of the climate change is the Semi-Distributional Soil & Water Assessment Tool (SWAT) which is an integrated, complex, basin-scale model capable of analyzing data annually, monthly, daily and hourly (Arnold et al. 1998). It was first presented by Dr. Jeff Arnold (Arnold 1994) for the United States Agricultural Research Service to predict the effects of management practices on water, sediment, and so on in large and complex basins with different land uses (Arnold et al. 1998; Shaigan et al. 2011; Neitsch et al. 2011).

To date, several studies have used SWAT to investigate runoffs; Alansi et al. (2009) used it to simulate runoffs to study the land-use variation effects upstream of Bernam basin in Malaysia. They used R^2 and Nash-Sutcliff (NS) impact coefficients to evaluate the simulated model and showed, through their results, that SWAT was highly capable of simulating and predicting runoff flows under humid tropical conditions.

Goyal et al. (2018) used SWAT in different DEMs to simulate runoff and sediment of the Narmada and Teesta fall basins in India and showed that different DEMs did not have meaningful effects on runoff results while their effects on the sediment simulation results were significant. Kaffas et al. (2018) used the Composite Mathematical Model (CMM) – Arc SWAT composite mathematical model for the modeling of hydro morphological processes in the Nestos river basin with an area of 840 km^2 in the mountainous part of Greece. They measured the discharge and sediment rates by SWAT and CMM methods and showed that composite model modeled sediments less accurately than CMM, but simulated runoffs satisfactorily.

Aiming at investigating the effects of climate on runoff, flood and drought downstream of Kan semi-arid watershed, west of Tehran, Ahmadi et al. (2019) used ANN, SWAT and IHACRES used ANN, SWAT and IHACRES to simulate rainfall and runoff under daily, monthly and annual scale for the period of 1987–1995. They suggested ANN and IHACRES because the basin lacked information and recommended SWAT for studying floods, runoffs and basin's physical properties. Chen et al. (2019) examined the effects of parameter uncertainty and structure of hydrological models in daily, monthly and annual land-use variation studies and simulated the Xitiaoxi Basin runoff in China using SWAT and HSPF hydrological models; the HSPF showed more monthly and annual runoff variations than SWAT. Differences in hydrological simulations could have been due to different equations used for both models. De Andrade et al. (2019) used SWAT to simulate the soil moisture and runoff in Brazil's northeastern basin. They examined the related uncertainty data in hydrometric stations and found NS coefficients of 0.71–0.92 and 0.53–0.76 for annual calibration and validation and 0.55–0.78 and 0.62–0.72 for monthly calibration and validation, respectively. Predicting the river discharge, where rainfall and air temperature are vital parameters, is an important issue in water resources engineering as regards the resource planning; in other words, the surface runoff discharge can be predicted by predicting the air temperature and rainfall (Khazaei and Mirzaei 2013) one method for which, for future time periods, is using statistical exponential micro-scale models. Some of the studies conducted, so far, on the effect of climate change on basins' runoffs using the predictions of exponential micro-scale models and simulations of the SWAT model are as follows: Liu et al. (2020) used SWAT to study the effects of climate change on the surface water in the South-Central Valley, California, for the year 2020. In this study, they used four climate models (Had-GEM-ESCMIP5, CNRM-CM5, CanESM2, Miroc5) and two emission scenarios (RCP4.5, RCP8.5) and showed, by their results, that the peak river flow was expected to increase 0.5–4 times in the coming decades under warm weather conditions and occur 2–4 months earlier in the year due to snow melting. They also concluded that in the near future (by the end of the twenty-first century), the snow cover would gradually decrease with lower rates at lower altitudes and with higher rates at higher altitudes. According to their predictions, the surface water would increase in the Valley, but increased time variations (more wet seasons and drier dry seasons) would cause new challenges for the supply management. They further emphasized that the remote measurement-based snow water equivalent (SWE) data could fill the current gap of the SWE observations in a limited area to improve the Swat snow setting and better predict the climate change effects

in semi-arid and snowy watersheds. Tan et al. (2017) used CMIP5 and SWAT models to study the Kelantan River catchment area in Malaysia. In this study that included 36 micro-scaled weather forecasts from 5 general circulation models (GCMs) under 3 RCP scenarios (2.6, 4.5, 8.5) in the SWAT calibrated model for the 2015–2044 and 2045–2074 periods, they showed that monthly rainfalls increased during wet seasons and reduced during dry seasons concluding that the monthly surface flows were likely to increase in November, December, and January and reduce slightly between June and October during the 2015–2044 period. These findings can serve as a scientific reference to develop better climate-adaptation strategies. Using a set of CMIP5 GCMs, Wodaje et al. (2021) evaluated the climate-change uncertainty effects on the Bilate River flood flow, Ethiopia, SWAT-simulated the water flow and showed, statistically, that the model predicted the flow logically. The annual discharge increased considerably for all time periods throughout the century; the flow increases under RCP8.5 scenario (compared to RCP4.5) was nearly 42.42% during the 2080 period. Andrade et al. (2021) used SWAT, two RCMs (Eta-Miroc5, Eta-HadGEM2) and two scenarios (RCP4.5, RCP8.5) to evaluate the future climate-change effects on Mundaú River Basin water resources, Brazil, for three time periods and showed, by climate models' predictions, that, in general, the Mundaú River Basin would experience significant annual rainfall reductions of between 0.4% (1,087.45 mm) and 25.3% (815.59 mm) in both scenarios, respectively.

Studies conducted so far on the effects of climate change on runoffs in mountainous basins are limited; however, none has addressed the prediction of the hydrological drought index in these basins. Therefore, this research is aimed to study the effects of the climate change on runoffs, evaluate the hydrological drought index and examine the flow trend in the Alvand mountain basin in Iran. To this end, SWAT and CMIP5 climate models were used to simulate the basin runoff and predict the climatic parameters, respectively. This study is mainly aimed to: (1) calibrate SWAT and do a daily-monthly runoff comparison of 4 hydrometric stations in the Alvand mountain basin, (2) predict the temperature and rainfall in 2020–2040 period in five meteorological stations and (3) simulate the runoff of four stations using the predicted data and calibrated parameters and compare the observed runoff with that predicted for future periods, (4) investigate the runoff trend using Mann–Kendall method and (5) evaluate the future hydrological drought index and compare it with that of the past.

2 Materials and methods

2.1 The study area

The Alvand mountainous basin, is located in Hamedan province and a sub-catchment area in the western part of Iran, which is formed along with the Zagros Mountain range, and its other name is Central Zagros with an area of 1133.62 km^2 along the longitude 48 · 36′to 48 · 7′North and the latitude 34 · 28′to 34 · 56′East. The minimum altitude in this area is 1582 and the maximum altitude is 3555 m above sea level Fig. (1).

Hamedan synoptic stations have reported 8.36, 6.9 and − 6.29 °C for, respectively, the absolute maximum, average and absolute minimum air temperature in the Alvand mountain basin; the warmest months are July and August (maximum 35 °C) and the coldest are January and February (average − 4.25 °C). Reports also show that the annual rainfall is more than 300 mm varying in different months with a maximum of 95 mm in April, 82 mm in May and 81 mm in June, and varying seasonally in other months (http://www.irimo.ir).

2.2 SWAT model

To simulate the runoff flow, this study has used SWAT which is a semi-distribution physical hydrological model designed to predict long-term runoffs, sedimentations and chemical-agricultural products in a watershed. It does the simulation of hydrological processes in two phases: (1) ground or soil profile and (2) routing, respectively (Arnold et al. 1998). Phase ground calculates the inflow of water, sediments, nutrients and pesticides to the main channel in each reservoir based on the water balance concept that considers such important processes as rainfall, ET, seepage, surface runoff, lateral flow and groundwater flow, and phase routing uses the main channel to connect all sub-basins and simulates the water and sediment movement towards the basin outlet (Cibin et al. 2010; Chen et al. 2019; Arnold et al. 1993; Gebremariam et al. 2014). In SWAT, interflow is calculated using a linear function that consists of slope length and angle, saturated conductivity, drainable porosity and the amount of water that is stored in the saturated zone (Cornelissen et al. 2013). SWAT simulates hydrological cycles based on the following water balance Eq. (1):

$$SW_t = SW_0 + \sum \left(R_{day} - Q_{surf} - E_a - W_{seep} - Q_{gw} \right)$$

(1)
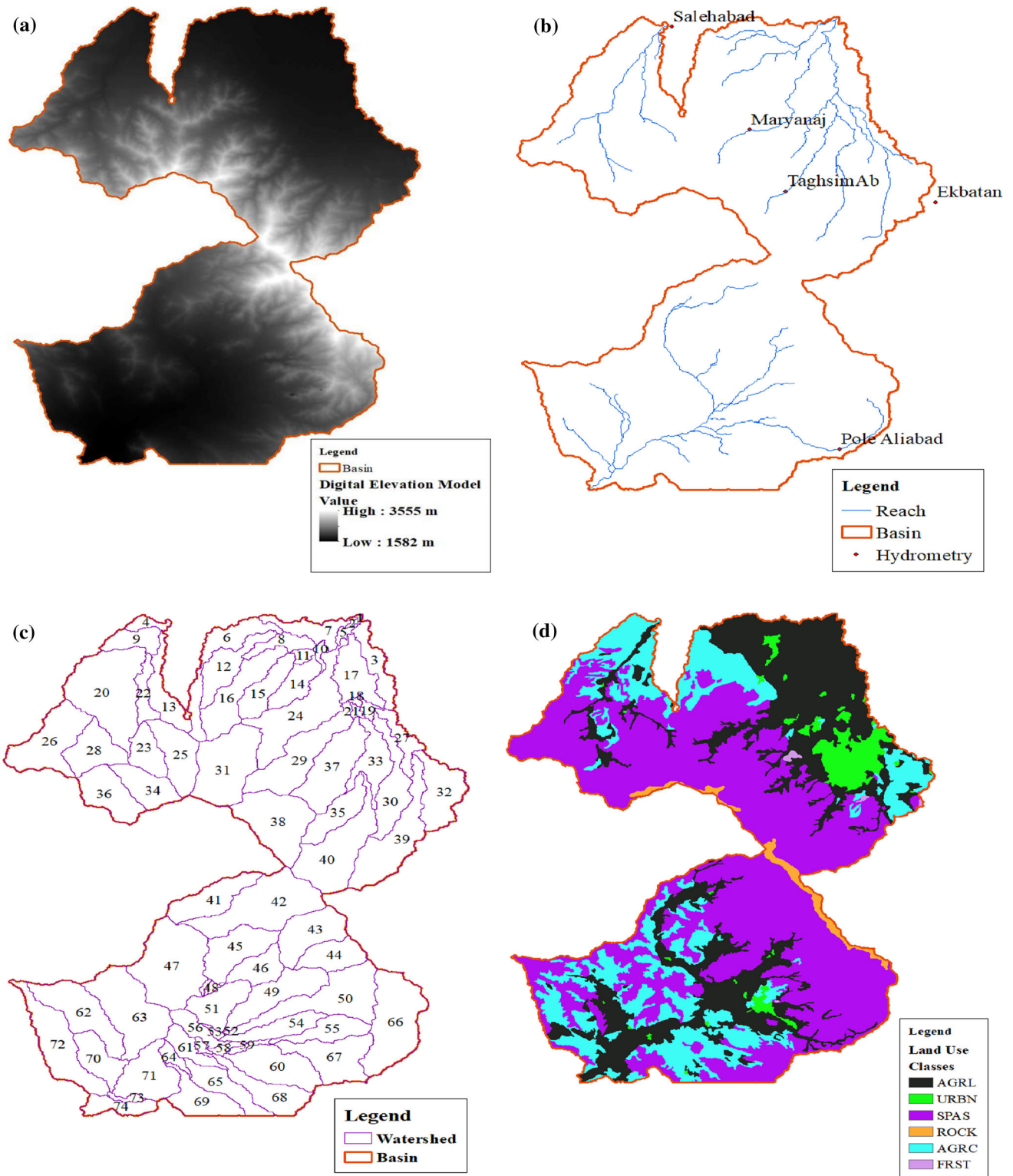
Fig. 2 **a** Digital elevation model of the study area, **b** Hydrometric stations and flow direction, **c** Division of Sub-basins, **d** Land use map

where SW_0 and SW_t (mm) are the initial and final soil water and R_{day}, Q_{surf}, E_a, W_{seep} and Q_{gw} (mm) are the rainfall, runoff, ET, water seepage to the upper soil layer and return flow in the ith day, respectively.

2.3 SWAT input data

SWAT uses the digital elevation model (DEM) and Raster primary functions through the Spatial Analyst feature in the

Table 1 Specifications of the stations used in the area

Station type	Station name	Latitude	Longitude	Elevation (m)	Data collection period
Synoptic	Tuyserkan	34.33	48.26	1783.2	2003–2017
Synoptic	Hamedan	34.51	48.32	1741.5	2003–2017
Hydrometric	Ekbatan	34.758	48.6	1935	2003–2017
Hydrometric	SalehAbad	34.924	48.338	1786	2003–2017
Hydrometric	Maryanaj	34.825	48.417	1979	2003–2017
Hydrometric	Pole Aliabad	34.515	48.514	2098	2003–2017
Hydrometric	TaghsimAb	34.766	48.45	2088	2003–2017

Table 2 Specifications of 4 models selected from the CMIP5 collection for the present study (IPCC 2013)

No.	Model	Institution/Country	Spatial resolution
1	GFDL-CM3	Geophysical Fluid Dynamics Laboratory, USA	2.5 × 2.0
2	EC_EARTH	EC_EARTH consortium published at Irish Centre for High End Computing, Netherlands/Ireland	1.28 × 2.5
3	Hadgem2_ES	Met Office Hadley Centre, UK	1.875 × 1.25
4	Miroc5	Atmosphere and Ocean Research Institute (The University of Tokyo), National Institute for Environmental Studies, and Japan Agency for Marine-Earth Science and Technology, Japan	1.41 × 1.39

ArcGIS software to design flow networks and basin boundaries (Abbaspour et al. 2007). To this end, the DEM10 map was first obtained from the Natural Resources Department (Section of Studies), Hamedan Province, and then used for modeling purposes (Fig. 2a). As the network of waterways and sub-basins was not previously identified, we formed it by the "flow direction and accumulation" technique and then examined it in the Google Earth software (Fig. 2b). This network and its basins were divided into 74 sub-basins (Fig. 2c). Since the provincial soil map did not exist, use was made of a global soil map and the land use map (Fig. 2d) was obtained from the mentioned Unit and introduced to the model in the GIS.

Characteristics of the measuring stations of the meteorological and runoff parameters in the study basin are listed in Table 1. In this catchment, there were two synoptic stations, Hamedan and Tuyserkan, that used the daily data on radiation, rainfall, air humidity, wind speed, and air temperature in the 2003–2017 period, and five hydrometric stations (Fig. 2b), Ekbatan, SalehAbad, Maryanaj, Pole Aliabad, and TaghsimAb, with the daily information in the same period obtained from the Water Resources Department; although Ekbatan Station was not inside the study area, its daily rainfall data were used because it was quite close to the area. Data introduction to the model should be regular with no blanks or else the model will become erroneous; here, the model received 65,700 meteorological data.

Performance of the mentioned model was studied and compared using such coefficients as: (1) Correlation, (2) NS, (3) PBIAS and (4) RMSE (Liu et al. 2021).

2.4 Future climate scenarios (climate forecast data)

To assess the climate change effects on runoffs as well as on the hydrological drought, the Lars-wg6 model was used to downscale and generate future daily rainfalls and temperature data through different general circulation models (GCMs). Two scenarios (RCP4.5 and RCP8.5) and 4 CMIP5 models (GFDL-CM3, Ec_Earth, Hadgem2_ES and Miroc5) were used to evaluate and model the rainfall and temperature of the 5 meteorological stations. While the first three represented the "average temperature and rainfall", "cold and humid climate" and "hot and dry climate", respectively, all 4 covered the CMIP5 model forecast results (Table 2).

Each CMIP5 model considered varying emission rates of solar greenhouse gases, human activities, volcanic eruptions, emission of short-term species, and natural/human aerosols known, also, as RCP-representing concentration routes. This study considered RCP4.5 and RCP8.5 emission scenarios of each CMIP5 model both of which are commonly used by researchers because RCP4.5 is an intermediate scenario while RCP8.5 is generally considered as the worst climate-change scenario (Liu et al. 2021). In short, to estimate the future runoff in SWAT, the mentioned models and scenarios.

2.5 Mann–Kendall trend test

In this study for investigate the trend of runoff Mann–Kendall test was used. The Mann–Kendall method explained briefly next.

In the MK (denoted by MK1) test, the first step is the calculation of the S statistics using the observations and employing the following Eq. (2) (Mann 1945; Kendall 1975):

$$Z = \sum_{i=1}^{n-1} \sum_{j=1}^{n} \text{sgn}(x_j - x_i) \qquad (2)$$

where x_j is the value of jth data, n is the number of data, and sgn (θ) is the sign function, which is defined as:

$$\text{sgn}(\theta) = \begin{cases} 1 & if & \theta \rangle 0 \\ 0 & if & \theta = 0 \\ -1 & if & \theta \langle 0 \end{cases} \qquad (3)$$

If $n > 8$, the S statistics has a normal distribution having E(S) = 0 and following variance:

$$V(s) = \frac{n(n-1)(2n+5) - t_i(t_i - 1)(2t_i + 5)}{18} \qquad (4)$$

where t_i is the number of observations in the ith tied class, and m is the total number of tied classes. The score of MK test or Z statistic is calculated as follows:

$$Z = \begin{cases} \dfrac{S-1}{\sqrt{V(s)}} & if & S \rangle 0 \\ 0 & if & S = 0 \\ \dfrac{S+1}{\sqrt{V(s)}} & if & S \langle 0 \end{cases} \qquad (5)$$

If the $(-Z_{1-\alpha/2} \leq Z \leq Z_{1-\alpha/2})$ condition is satisfied, H_0 (null hypotheses) is accepted, which means there is no significant trend in the tested time series; otherwise, H_1 (alternative hypothesis) is accepted, which means there is a significant trend in time series at α significance level.

2.5.1 Sen's estimator

In this study, the magnitude of trends is calculated using the Sen's estimator (Theil 1950; Sen 1968) method using the following Eq. (6):

$$\beta = Median\left(\frac{x_i - x_j}{i - j}\right) \quad \forall_j \langle i \qquad (6)$$

where x_j and x_i are the jth and ith observations in the tested time series. The positive values of β represent the upward trends, whereas the negative values indicate the downward trends.

2.6 The streamflow drought index (SDI)

For determination of the severity and weakness of hydrological drought, an index similar to standardized rainfall index (SPI) called streamflow drought index (SDI) is used. This index is based on the monthly standard normal flow

and was first introduced by Nalbantis and Tsakiris (2009). In the present study, SDI was calculated using a method completely similar to SPI (McKee et al. 1993). Therefore, for calculating this index, the same calculations were made except that discharge monthly series were used instead of rainfall data as the input. Accordingly, first, the time window was introduced for the monthly series of river discharge. The time window shows the multi-monthly cumulative value of the river flow discharge. For example, the 3-month time window of June-2014 is the cumulative value of the streamflow values of the months April, May, and June of 2014 or the 12-month time window of June-2014 is the monthly cumulative streamflow values of July-2013 to June-2014. A cumulative monthly time window is derived based on the following equation:

$$V_{i,k} = \sum_{j=1}^{3k} Q_{i,j}; \quad i = 1, 2, \ldots; \quad j = 1, 2, \ldots 12;$$
$$k = 1, 2, 3, 4 \qquad (7)$$

where $V_{i;k}$ is the cumulative streamflow value of the kth monthly period in ith hydrological year, j denotes the month within the hydrological year and $Q_{i;j}$ is the monthly streamflow (Myronidis et al. 2018; Tabari et al. 2013). After this step, by comparing different probability distributions, the fittest distribution was applied on the data in each of the time windows and the probability corresponding to each average discharge value was calculated. Subsequently, based on the principle of distribution transformation, the mentioned probability was transformed into standard normal distribution and new series of data were obtained that had a standard normal distribution with a mean of zero and a variance of 1. The SDI calculation

$$SDI_{i,k} = \frac{v_{i,k} - \overline{v_k}}{s_k} \qquad (8)$$

where $\overline{v_k}$ and S_k are the mean and standard deviation of the cumulative streamflow volumes, $SDI_{i;k}$ is the value of streamflow drought index for kth monthly-based time window (Malik et al. 2019; Borji et al. 2016). According to Table 3, the severity and weakness of hydrological drought (or wet) condition, can be classified in the resulting series.

The present study's general flowchart is shown in (Fig. 3).

3 Result

3.1 Calibrated parameters

The calibration step of a hydrological model is subjective and no automatic algorithm can replace the researcher's knowledge in relation to their study area. Therefore, the

calibration procedures and uncertainty analysis are closely connected, and no calibration should be performed without quantifying the degree of uncertainty associated with the model prediction (Abbaspour et al. 2015; de Andrade et al. 2019).

Table 3 Classification of hydrological drought severity for stream flow Drought Index

SDI value	Class
2 <	Extreme wet
1.5 to 2	Severe wet
1 to 1.5	Moderate wet
− 1 to 1	Normal
− 1.5 to − 1	Moderate drought
− 2 to − 1.5	Severe drought
− 2 >	Extreme drought

This study has used period of 2003 to 2008 as the Warm up period (because these 6 years had high positive effects on the authors' statistical results), 2009–2014 for calibration and 2015–2017 for validation. As the study basin was mountainous and obtaining results was quite difficult, input parameters were considered separately for each sub-basin, which were totally 74 and similar ones were placed in one direction so that instead of setting one parameter for every sub-basin and finding an optimal value for it, only one was obtained for similar sub-basins that were totally 12; same was repeated for the soil map. Parameters used to simulate monthly and daily runoffs, their description and their calibrated values are listed in Table 4.

In the present study, the Alvand mountain basin has 6 types of land use, and 3 types of soil. In this range, the hydrological group of the basin soils is in the B and C groups according to the soil permeability, i.e. the permeability of the range is between 3.8 to 7.5 (mm per hour). Besides the characteristics of the basin's surface cover are
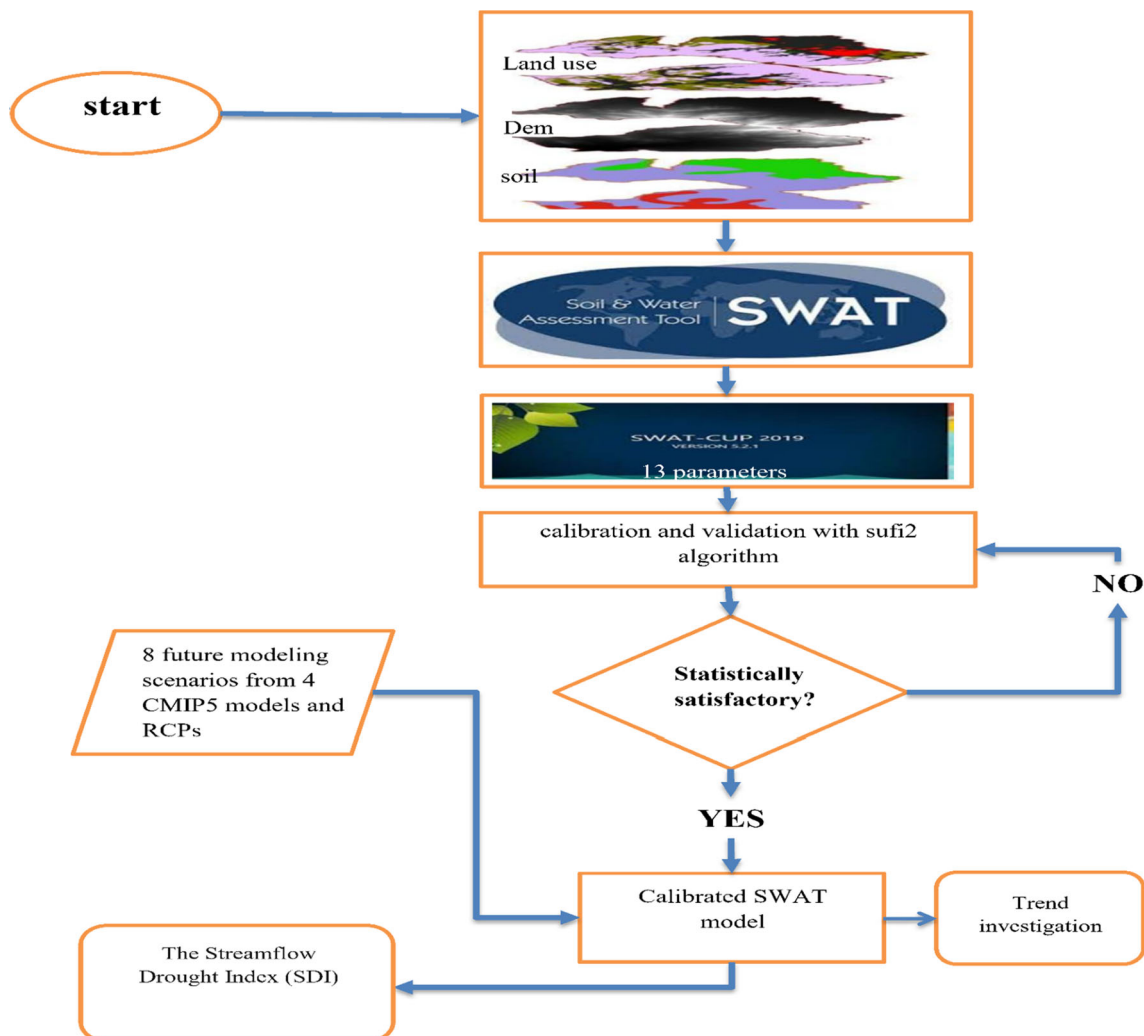

Fig. 3 The proposed modeling framework

Table 4 SWAT model parameters' calibrated and adjusted values

No.	Parameter	Description	Initial range	Calibrated value
1	CN2	Curve Number, moisture condition II	30–90	35–98
2	ALPHA_BF	Baseflow alpha factor (days)	0–1.0	0/0403
3	GW_DELAY	Groundwater delay, days	0–500	34.9778
4	GWQMN	Depth of water in shallow aquifer required for return flow, mm	0–5000	239.961
5	HRU_SLP	Average slope steepness	0–1.0	1.610
6	RCHRG_DP	Deep aquifer percolation fraction	0–1.0	0.9
7	SLSUBBSN	Average slope length	10–150	94.4244
8	SURLAG	Surface runoff lag time	1–24	12.985
9	CH_N2	Manning's ''n'' value for the main channel	0.016–0.2	0.0627
10	CH_K2	Effective hydraulic conductivity in main channel alluvium	− 0.01–500	67.585
11	SOL_AWC	Available soil moisture capacity, mm mm_1	− 0.6–0.6	− 0.13–0.58
12	SOL_K	Saturated hydraulic conductivity, mm h_1	0–2000	123.686–1159.6
13	SOL_BD	Moist bulk density	0.9–2.5	1.302–2.24

arable lands, grasslands, gardens or forests, there are also unused areas which are bare, urban, rocky and mountainous. In our study, the calibrated value of the curve parameter (CN) for 12 similar sub-basins ranged from 35 to 98, where high CN values show the low permeability of the soil and therefore more runoff. Parameters obtained in this basin show different soil types and land uses. While this calibration results for the CN parameter is consistent with those of Lin et al. (2014), the related values obtained in de Andrade et al. (2019), Zettam et al. (2017) and Hammouri et al. (2017) studies ranged from 35 to 98. The value of the Baseflow alpha-factor (ALPHA_BF) varied from 0 to 1 day, with a calibrated value of 0.040, which was consistent with the results of de Andrade et al. (2019) and Fereidoon et al. (2019). Groundwater delay time (GW_DELAY) can vary from 0 to 500 days, which is the default limit provided by the SWAT model. In this study basin, the calibrated value (with 1333.62 km^2) was approximately 35 days, while de Andrade et al. (2019), recorded 135 days in the Mundaú River basin (with an area of 4090.39 km^2), as well as Xue et al. (2014) in China (with an area of 8,102 km^2) obtained a calibrated value of 101 days whilst analyzing the surface current uncertainty parameter and sediment production in the Huolin Basin. On the other hand, Blainski et al. (2017) recorded a value of 0.65, indicating that the time interval required for underground feeding in the Camboriú River Basin (195 km^2) was less than one day. These differences emphasize the significant role of drainage zone size in the GW_DELAY

parameter. The water depth in shallow aquifers required for return flow (GWQMN) can vary from 0 to 5000 mm. The return flow from groundwater is related to rainfall and particularly evapotranspiration, since it is strongly dependent on capillary flow. A calibrated value of 239.9 mm indicates that the water level must be equal to or greater than approximately 0.24 m in depth for the return flow in the catchment areas of the region. de Andrade et al. (2019) obtained the GWQMN parameter value of 2686 mm.

The HRU_SLP (Average slope steepness) calibration mean value of was 1.61 in this study, which was essentially 61% of the initial value of each subset. The permissible value of RCHRG_DP deep aquifer percolation fraction varies between 0 and 1%. Its calibrated value for the total sub-basin is 0.9 Fereidoon et al. (2019) obtained the RCHRG_DP value in the Karkheh Basin of Iran between 0.25 and 0.64. Bhatta et al. (2019) obtained this value in the Tamor River Basin in Nepal 0.56. The Average slope length of the SLSUBBSN slope is between 10 and 150, and in this study, it was 94.42. Surface runoff lag time coefficient (SURLAG) can alter from 1 to 24, the calibrated value in this area was 12.985. Semiromi and Koch (2019) obtained the SURLAG value in the Gharehsoo River basin in Iran at 3.63. Bhatta et al. (2019) obtained this value in the Tamor River basin in Nepal 0.56. Aliyari et al. (2019) obtained the calibrated amount of SURLAG for the Pallet River Basin in Colorado at 6,985. The calibration value of the manning coefficient (CH_N2) was 0.062 in this study, which shows the effluents in the heavy clay-silty soil are

almost uniform with the floor and the cross section of the effluents (Chow and Patterson 1959). de Andrade et al. (2019) found the calibration value of CH_N2 to be 0.34, and the main features of this channel are very grassy, torrential streams with heavy wood and plant bases. Rajib et al. (2016) found adjusted values CH_N2 from 0.02 to 0.15 in the studied basins. Zhang et al. (2015) obtained this parameter in the Jinjiang River Basin in China at 0.03. Pereira et al. (2014) obtained the CH_N2 value of the Headwater basin in southern Brazil at 0.011. The calibrated value of the CH_K2 Effective hydraulic conductivity in main channel alluvium in this study was 67.57.

For calibration of the Available soil moisture capacity (SOL_AWC), values can vary from -60% to $+60\%$. This value varies from 0.04 to 0.12 mm/mm for different soil types. The calibrated value of SOL_AWC for the 5 similar sub-basins decreased from $+58\%$ to -13%. The highest is between 0.063 mm/mm and 0.19 mm/mm and the lowest is between 0.0348 mm/mm and 0.1044 mm/mm.

de Andrade et al. (2019) indicated that the SOL_AWC value for all soils between 0.053 mm/mm and 0.158 mm/mm. Aliyari et al. (2019) obtained the calibrated value of SOL_AWC for the Pallet River Basin in Colorado at 0.9136. Chen et al. (2019) obtained the calibrated value of SOL_AWC between 0.025 and 0.35. The calibration value of saturated hydraulic conductivity (SOL_K) in this study was between 123.68 and 1159.6 for pasture and basin coverage. According to Andrade et al. (2013), saturated hydraulic conductivity usually presents a high spatial variability, and the SWAT model does not take into account this spatial distribution but, rather, a mean value for a given soil type. Then, the model provides, from the optimization process, the maximum value allowed in the calibration step.

The Moist bulk density (SOL_BD) varies from -50% to $+50\%$. This amount has increased to 222 percent for the same 5 sub-basins and also decreased to 14 percent. Fereidoon et al. (2019) obtained SOL_BD values in the Karkheh basin of Iran between 0 and 0.23.

3.2 Calibration and validation of SWAT

Comparison between the simulated and observed hydrographs is an important procedure to evaluate model calibration (Andrade et al. 2013; Blainski et al. 2017). Figures 4 and 5 show the hydrographs observed and simulated by the SWAT model, in the calibration and validation phases, for the four streamflow gauge stations of the

Alvand mountain Basin (SalehAbad, Tooijin, TaghsimAb and Pole Aliabad) for daily and monthly time steps, respectively. For both time steps, a satisfactory fitting between measured and simulated hydrographs was observed. The model has simulated the studied area well, but has been relatively erroneous in simulating the runoff peak.

Table 5 shows the comparison among the statistical indicators (R^2, NS and PBIAS) for discharge calibration and validation using the SWAT-CUP semiautomatic calibration method. Values of R^2 ranged from 0.48 to 0.76 for daily and monthly flow calibration, and from 0.38 to 0.70 for validation; as shown, the difference between the two is not much. The NS coefficient ranged from 0.4 to 0.7 for monthly calibration and from 0.4 to 0.52 for daily calibration; the reason for less daily accuracy factor than monthly is that the data calibrated daily at each station are 2922, but for the monthly case they are 96. According to the NRMSE coefficient that shows the percent error, the highest calibration and validation error rates are, respectively, 17.5 and 19.7% for the monthly data of the TaghsimAb, and the lowest are, respectively, 8 and 48.47% for the daily data of Maryanaj station. These results show that, in general, the SWAT performance is good and satisfactory for rivers flowing from the Alvand mountain basin based on Moriasi et al. (2007) proposed classification.

3.3 Evaluating the rainfall and temperature parameters and simulating the future runoff

The statistical data, including the daily rainfall for Hamedan, Tuyserkan, SalehAbad, Maryanaj and Ekbatan stations and the minimum and maximum temperatures for Hamedan and Tuyserkan stations were gathered in period of 2003 to 2017, then used as input Lars-wg model to simulate future rainfall and temperature based on the CMIP5 models for period of 2020 to 2040.

Table 6 lists the R^2, NS, PBIAS, RMSE and NRMSE error criteria for the selected models. The results show that Miroc5, with the lowest error, is the best model to predict the rainfall and temperature in the study area. The R^2 and NS coefficients obtained in simulating meteorological station data by Miroc5 model with RCP8.5 scenario have values above 0.9, which are good results, and the RMSE coefficient shows that the rainfall and the minimum and maximum temperatures are, in a monthly scale, erroneous by about 2.81, 0.17 and 0.29 mm, in Hamedan station, 4.32, 0.27 and 0.21 in Tuyserkan station and 5.52, 4.42 and 3.82 in Ekbatan, SalehAbad and Maryanaj stations,

Fig. 4 Comparison of the simulated daily runoffs with those observed in SalehAbad, TaghsimAb, Maryanaj and pole Aliabad stations

respectively. In Hamedan station, the rainfall and, the minimum and maximum temperatures are erroneous by 5.3, 0.8 and 0.9%, in Tuyserkan station these values are

5.4, 1.2 and 0.7% and in Ekbatan, SalehAbad and Maryanaj stations they are 8.6, 8.3 and 7.2%, respectively.

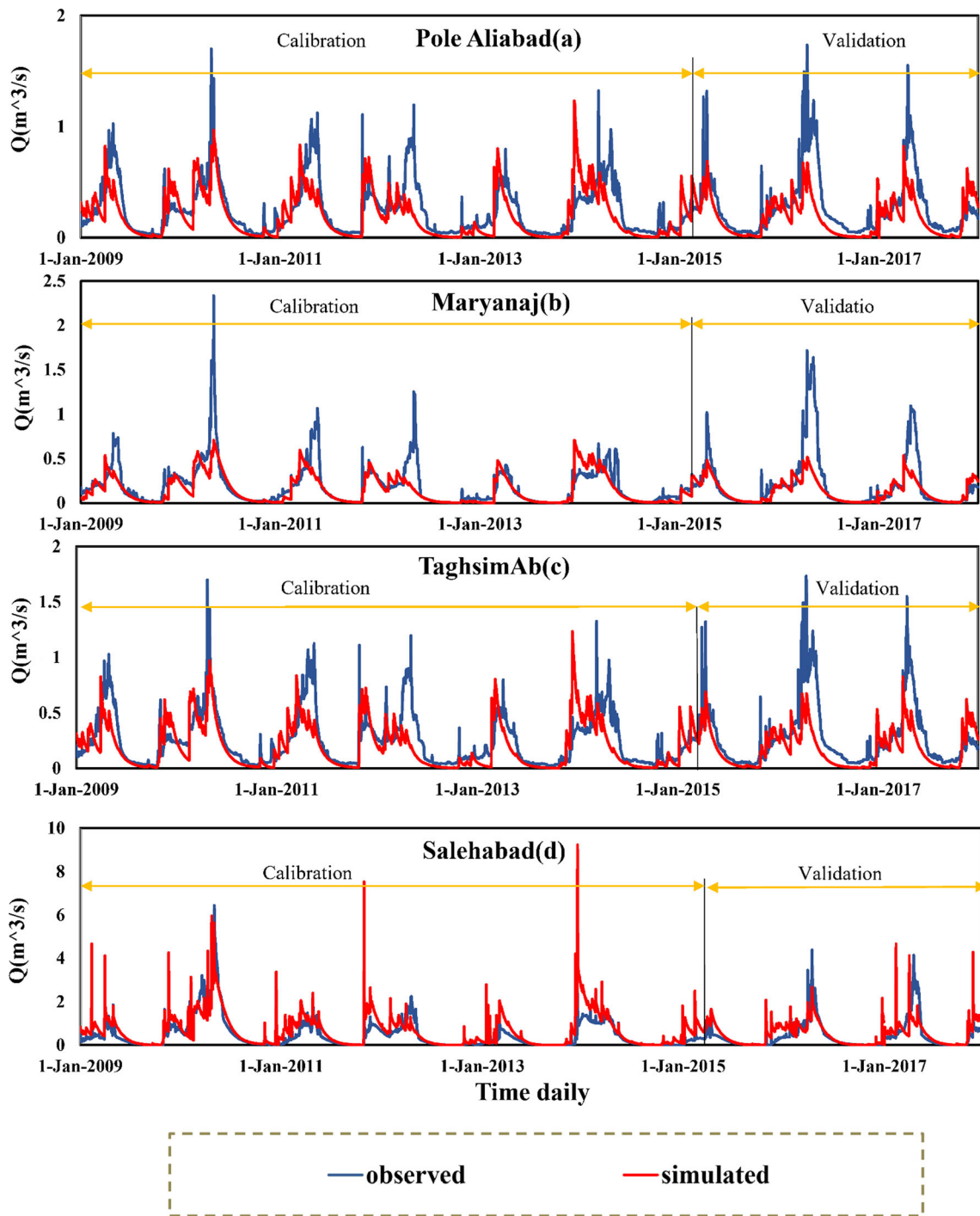The average monthly rainfall and, the minimum and maximum temperatures of the five meteorological stations,
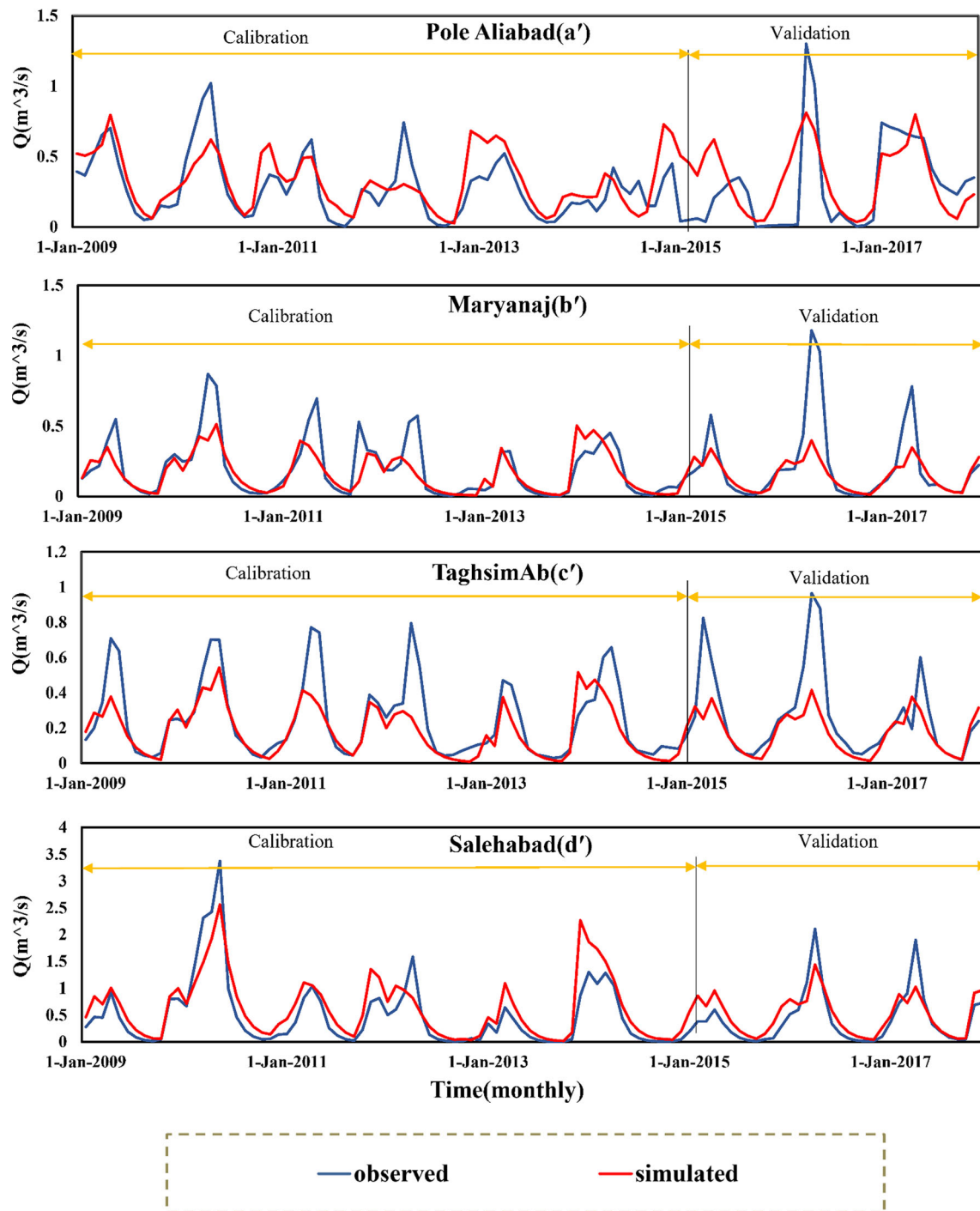
Fig. 5 Comparison of the simulated monthly runoffs with those observed in SalehAbad, TaghsimAb, Maryanaj and pole Aliabad stations

which simulated by the outputs of the CMIP5 model (Miroc5) with the RCP8.5 scenario in period of 2020–2040, are shown in Fig. 6. Where the rainfall is the lowest in June to September (dry season) and the temperature is, contrarily, at its maximum possible.

Figure 7 shows the predicted runoff with SWAT for Pole Aliabad, Maryanaj, TaghsimAb and SalehAbad stations under CMIP5 models (GFDL-CM3, EC_EARTH, Hadgem2_ES, Miroc5) and two scenarios (RCP4.5 and RCP8.5). According to the Fig. 7, it can be concluded that the predicted runoff under Miroc5 model is more than runoff under other models in all the stations. But, the lowest predicted runoff in the study area is under GFDL-CM3 model.

Table 5 A summary of the daily and monthly time step calibration and validation of the SWAT model statistics in the four streamflow gauge stations of the Alvand mountain basin

Statistics	SalehAbad		Maryanaj		TaghsimAb		Pole Aliabad	
	Daily	Monthly	Daily	Monthly	Daily	Monthly	Daily	Monthly
Calibration								
R^2	0.66	0.76	0.52	0.55	0.48	0.65	0.51	0.52
NS	0.52	0.7	0.47	0.50	0.40	0.50	0.41	0.42
PBIAS	−18.6	−30.8	12.5	19.8	36.9	29.8	15.6	−26.0
RMSE	0.450	0.317	0.187	0.165	0.188	0.167	0.217	0.202
NRMSE	7.00%	9.44%	8.00%	14.08%	10.87%	17.5%	10.89%	15.89%
Validation								
R^2	0.47	0.70	0.55	0.46	0.45	0.44	0.56	0.38
NS	0.47	0.68	0.44	0.46	0.36	0.44	0.38	0.38
PBIAS	14.3	4.2	6.7	20.3	11.8	5.0	12.5	22.6
RMSE	1.274	0.28	0.529	0.159	0.532	0.114	0.615	0.148
NRMSE	30.80%	15.37%	48.47%	21.13%	34.47%	19.70%	18.58%	21.73%

The Z statistical values for Pole Aliabad, TaghsimAb, Maryanaj and SalehAbad stations simulated under RCP4.5 and RCP8.5 scenarios are listed in Table 7 where the runoff from 2020 to 2040 has a positive trend in most stations under different scenarios, but has no significant trend in 90, 95 and 99% probabilities in any of the stations; the highest runoff increase belongs to RCP4.5 and RCP8.5 scenarios in SalehAbad station with the GFDL-CM3 model. In Table 8 that shows the S statistical values of the trend line slope criterion, the highest slope belongs to SalehAbad station (1.46) for the GFDL-CM3 model under RCP4.5 and RCP8.5 scenarios; this slope is positive showing a runoff increase, but only a little.

To check the uncertainty range of the present study's climate change models on runoffs resulting from the SWAT model, first their outputs were produced in the form of monthly average temperature and rainfall, then their differences were calculated (for each model) using the average of the base period and their variations were plotted as box diagrams and, finally, the box plot resulting from the runoff output of the SWAT model, which is under the temperature and rainfall of climate change models, was drawn. Figure 8 shows the box plot of the temperature and rainfall predicted by Miroc5 model with RCP8.5 scenario, which was the best model for the study area. As shown, rainfall variations are high in wet season and low in dry season (Jun, July and August). The highest variations belong to Ekbatan Station in October; the highest/lowest coefficient of temperature variations relate to the months of winter/summer. In Fig. 9 that shows the box plot of the runoff predicted by SWAT model under the Miroc5 climate change model with the RCP8.5 scenario, an increase in the coefficient of rainfall/temperature variations in wet seasons also increases the coefficient of the variations of the runoff simulated with the SWAT model, but in dry

seasons (June, July, Aug. and Sept.), runoff variations are more than the temperature and rainfall variations; most variations belong to the TaghsimAb Station in Dec. and June.

Table 9 shows the percentage of predicted runoff variations in the period of 2020–2040 compared to the period of 2003–2017 under the CIMIP models. As shown, under Miroc5 (RCP8.5) model, the surface runoff in Pole Aliabad, Maryanaj, TaghsimAb and SalehAbad hydrometric stations is, respectively, 6.55, 2.56, 12.69 and 11.65% less in period of 2020–2040 compared to 2003–2017. The largest decrease in runoff in the period of 2020–2040 compared to the period of 2003–2017 is related to the GFDL-CM3 (RCP8.5) model (75.68%). As whole, under all models, the amount of average runoff decreases compared to the past.

Table 10 shows the runoff variations in all seasons in compared to the past under the models; as shown, the runoff under Miroc5 (RCP8.5) model increases in the basin by 99% and 165% in autumn and summer in compared to the past, respectively, but in the spring, runoff decreases by 67%. The highest runoff reductions found by GFDL-CM3 model under RCP4.5 and RCP8.5 scenarios are, respectively, − 60% and − 69% for winter. For spring, too, the highest reduction is related to the same model under the same scenarios, but for summer, it is related to Hadgem2_ES model with the same scenarios and amount, respectively, to − 79% and − 40%. Among all seasons, the highest runoff reduction, compared to the past, is − 75% for autumn. As whole, on a seasonal scale under all models, the amount of runoff decreases compared to the past, except under the scenario of RCP4.5 in the fall season which is unchanged (0%).

Table 11 shows the runoff variations in all months in compared to the past under the selected models; as shown,

Table 6 Summary of Alvand mountain basin model statistics with RCP8.5 and RCP4.5 scenarios

Statistics	Hamedan			Tuyserkan			Ekbatan	SalehAbad	Maryanaj
	Rain	Temp. (min)	Temp. (max)	Rain	Temp. (min)	Temp. (max)	Rain	Rain	Rain
GFDL-CM3 (RCP4.5)									
R^2	0.89	0.9	0.89	0.9	0.87	0.77	0.87	0.86	0.89
NS	0.8	0.5	0.7	0.7	0.6	0.6	0.5	0.5	0.6
PBIAS	−282.0	−402.4	555.2	−438.1	−244.5	538.3	−413.5	−493.9	−390.3
RMSE	11.38	7.51	4.16	16.29	6.44	4.85	13.19	14.45	12.82
NRMSE	16.70%	35.50%	14.90%	20.20%	19.15%	25.10%	20.40%	22.80%	19.60%
GFDL-CM3 (RCP8.5)									
R^2	0.86	0.91	0.7	0.89	0.91	0.77	0.91	0.86	0.83
NS	0..5	0.5	0.7	0.6	0.6	0.6	0.6	0.5	0.4
PBIAS	−525.8	−532.9	−85.2	−423.2	−424.6	−244.5	512.2	−358.1	−549.7
RMSE	14.65	15.81	5.80	4.77	18.34	6.58	4.37	13.83	15.63
NRMSE	29.70%	23.20%	22.20%	25.20%	28.00%	23.00%	12.70%	21.40%	27.20%
EC_EARTH (RCP4.5)									
R^2	0.96	0.9	0.86	0.93	0.93	0.83	0.76	0.82	0.85
NS	0.9	0.7	0.7	0.7	0.9	0.5	0.4	0.4	0.5
PBIAS	−104.4	−351.1	−241.5	373.4	−48.1	−344.1	−1210.0	−580.3	−549.8
RMSE	4.65	12.062	5.516	3.77	7.53	7.47	5.53	15.6	15.25
NRMSE	70.00%	20.00%	21.10%	13.00%	8.80%	27.00%	29.20%	31.40%	30.00%
EC_EARTH (RCP8.5)									
R^2	0.95	0.87	0.91	0.89	0.98	0.9	0.93	0.85	0.96
NS	0.9	0.6	0.8	0.8	0.7	0.8	0.8	0.5	0.9
PBIAS	−130.7	−139.1	−155.1	−124.9	−426.9	−123.9	657.9	−415.2	−114.4
RMSE	6.14	13.96	4.28	4.74	14.48	4.53	3.53	13.41	4.96
NRMSE	9.20%	16.90%	16.10%	17.90%	22.10%	15.90%	11.90%	20.80%	7.50%
Hadgem2_ES (RCP4.5)									
R^2	0.89	0.81	0.87	0.97	0.95	0.82	0.92	0.96	0.77
NS	0.7	0.6	0.7	0.5	0.6	0.7	0.6	0.6	0.6
PBIAS	−322.5	−376.1	270.83	838.5	−535.9	−200.3	1246.4	−519.8	−307.8
RMSE	12.01	14.28	5.81	5.00	17.707	5.89	4.68	12.7	12.59
NRMSE	18.00%	21.80%	18.00%	17.80%	25.10%	17.70%	16.00%	25.30%	18.90%
Hadgem2_ES (RCP8.5)									
R^2	0.89	0.89	0.86	0.87	0.93	0.91	0.89	0.87	0.97
NS	0.5	0.7	0.7	0.6	0.7	0.7	0.6	0.5	0.6
PBIAS	−532.6	−376.2	−179.9	−352.4	−425.9	−145.1	538.3	−413.6	−396.4
RMSE	14.9	12.61	5.26	4.66	15.53	6.07	4.85	13.14	12.42
NRMSE	23.70%	21.60%	16.90%	20.30%	19.20%	18.00%	25.10%	26.40%	18.60%
Miroc5 (RCP4.5)									
R^2	0.92	0.93	0.96	0.95	0.93	0.98	1.00	0.97	0.9
NS	0.9	0.9	0.9	0.9	0.9	1.00	1.00	1.00	0.8
PBIAS	−104.35	−140.83	−70.51	93.93	−48.02	−45.52	20.18	−80.14	−213.28
RMSE	6.89	7.417	2.64	2.21	7.54	1.72	0.377	4.09	8.29
NRMSE	10.40%	10.90%	10.10%	7.40%	8.80%	6.00%	1.60%	6.30%	11.90%
Miroc5 (RCP8.5)									
R^2	0.94	0.94	1.00	1.00	0.97	1.00	1.00	0.98	0.97
NS	0.9	0.9	1.00	1.00	1.00	1.00	1.00	1.00	1.00
PBIAS	−23.67	38.16	0.49	11.25	−15.52	−4.17	−5.4	−88.0	−88
RMSE	4.42	5.52	0.21	0.27	4.32	0.29	0.17	2.81	3.82

Table 6 (continued)

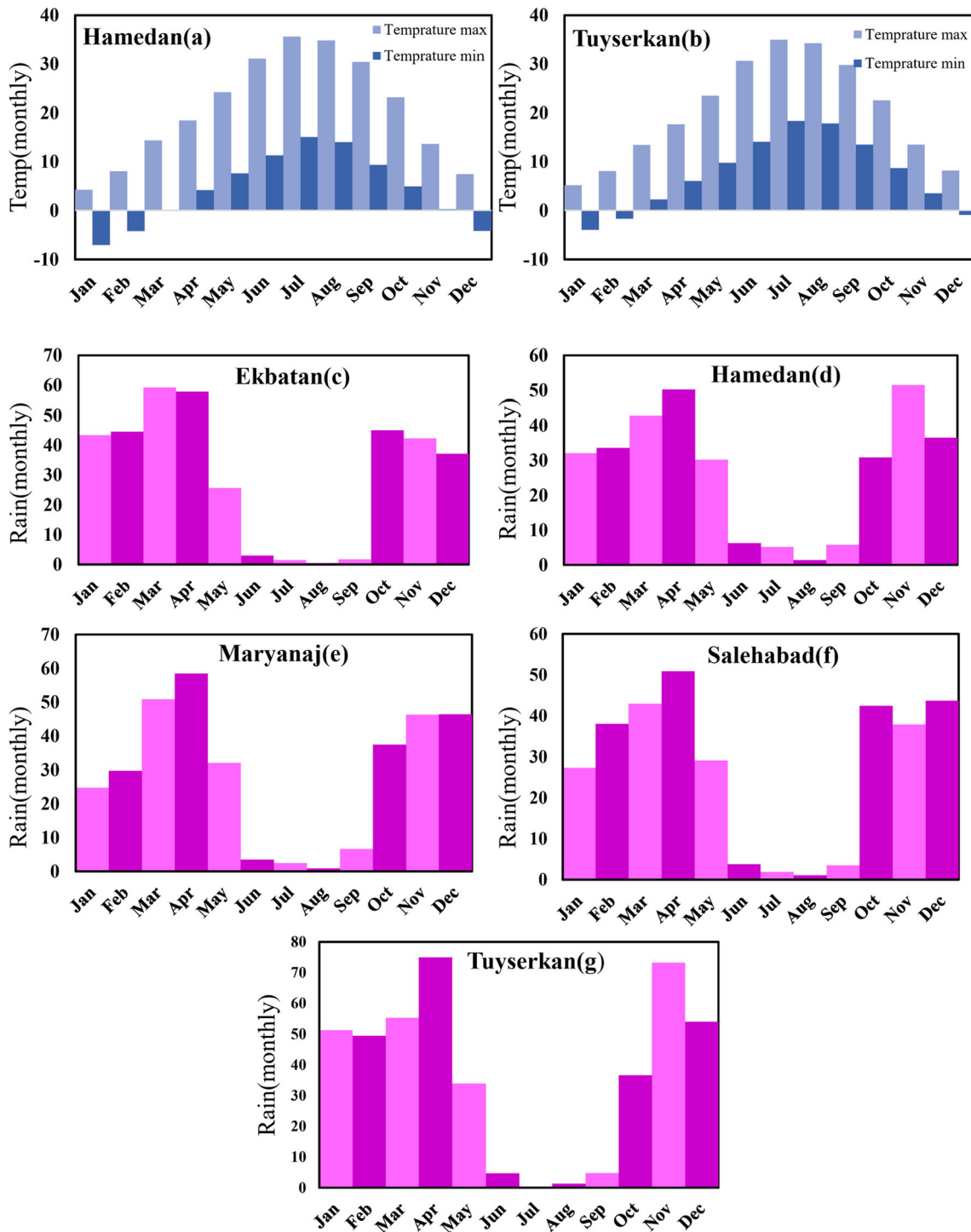| Statistics	Hamedan			Tuyserkan			Ekbatan	SalehAbad	Maryanaj
	Rain	Temp. (min)	Temp. (max)	Rain	Temp. (min)	Temp. (max)	Rain	Rain	Rain
NRMSE	8.30%	8.60%	0.70%	1.20%	5.40%	0.90%	0.80%	5.30%	7.20%

Fig. 6 Average monthly rainfall and the minimum and maximum temperatures (2020–2040)
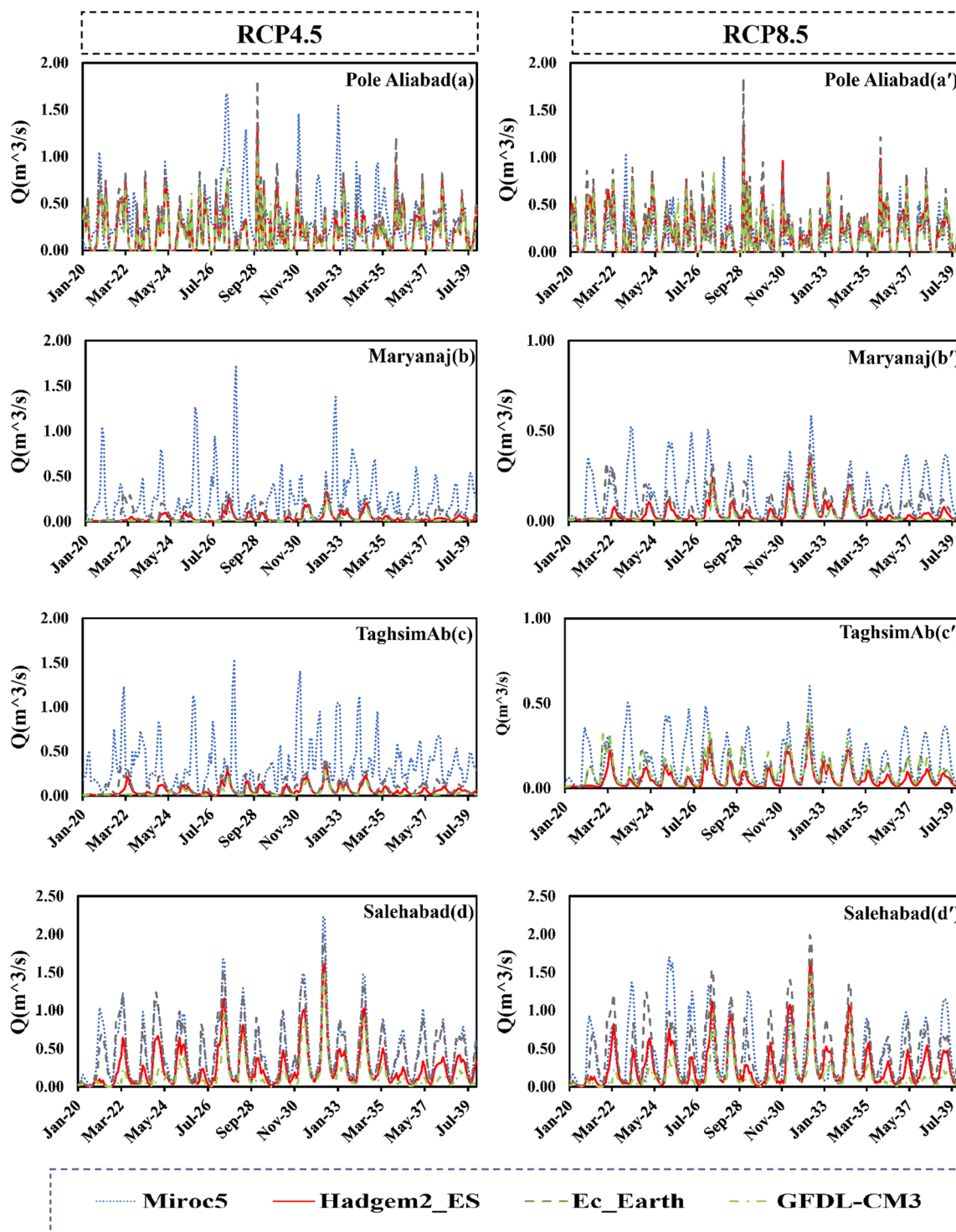
Fig. 7 Runoff simulated with CMIP5 model for SalehAbad, TaghsimAb, Maryanaj and pole Aliabad stations during 2020 to 2040

the highest average increase of runoff in the basin is by 222% under selected models, in September, but the highest average decrease is 78% in April. Among the models, the GFDL-CM3 model shows the highest reduction of runoff under the RCP8.5 scenario in April (87%) which this

reduction is 73% under Miroc5 (RCP8.5) model. Also, between the models, Miroc5 (RCP8.5) shows the highest increase of runoff in the basin, in September equal to 1102%.

Table 7 Statistical values of Z for SalehAbad, TaghsimAb, Maryanaj and Pole Aliabad stations

Z	Pole Aliabad	TaghsimAb	Maryanaj	SalehAbad
RCP8.5				
Miroc5	0.03	0.49	−0.03	0.36
Hadgem2_ES	−0.29	1.07	1.33	1.07
EC_EARTH	−0.16	0.75	1.46	0.49
GFDL-CM3	−0.36	1.14	0.68	1.46
RCP4.5				
Miroc5	0.03	0.00	−0.03	0.03
Hadgem2_ES	−0.36	1.14	1.33	1.07
EC_EARTH	−0.62	0.75	1.46	0.49
GFDL-CM3	−0.62	0.75	1.07	1.46

Table 8 Statistical values of S (trend line slope) for SalehAbad, TaghsimAb, Maryanaj and Pole Aliabad stations

S	Pole Aliabad	TaghsimAb	Maryanaj	SalehAbad
RCP8.5				
Miroc5	0.004	0.032	−0.004	0.014
Hadgem2_ES	−0.011	0.019	0.010	0.004
EC_EARTH	−0.013	0.009	0.019	0.040
GFDL-CM3	−0.006	0.007	0.001	0.042
RCP4.5				
Miroc5	0.006	0.000	−0.003	0.017
Hadgem2_ES	−0.013	0.019	0.013	0.092
EC_EARTH	−0.011	0.009	0.019	0.04
GFDL-CM3	−0.013	0.009	0.001	0.042

Figure 10 shows the SDIs in period of 2003–2017 for Pole Aliabad, Maryanaj, TaghsimAb and SalehAbad stations using the log normal distribution; the average SDI was normal for TaghsimAb and Maryanaj stations in the 2003–2017 period. A severe drought encountered for Pole Aliabad station in the 2008–2015 period and a moderate drought (−1.01) for SalehAbad station in the period of 2003–2017.

The SDI predicted for the 2020–2040 period is shown in Fig. 11. Pole Aliabad station face severe drought (−1.84) under the Miroc5 model with scenarios of RCP4.5 and RCP8.5, other models had normal values in this station. At the Maryanaj station, SDI shows normal (−0.06) under Miroc5 (RCP8.5) model and mild drought for other models under RCP4.5 and RCP8.5 scenarios; this station will face extreme drought (−3.88) in 2022 under Miroc5 model with

RCP4.5 scenario. As whole, at TaghsimAb and SalehAbad stations, the SDI under all models showed mild drought, But under the GFDL-CM3 model, the SalehAbad station experiences extreme droughts in 2026 (−4.35) and 2021 (−4.28). Also, TaghsimAb station faces extreme droughts in 2025 and 2026 under Miroc5 (RCP8.5) model.

Table 12 shows the percentage of SDI variations in period of 2020–2040 compared to 2003–2017 in the basin for under the selected models. As shown, the drought intensity in the Alvand basin will increase under all scenarios (126%). The highest increase of SDI occurs under Miroc5 (RCP8.5) model (180%) and the lowest increase of SDI (77%) occurs under Hadgem2_ES (RCP4.5) model in the basin. In stations of Pole Aliabad, Maryanaj, TaghsimAb, and SalehAbad, the average of highest increase of SDI under the all models is in the months of January (5505%), December (125%), January (201%), and December (100%), respectively.

4 Discussion

In studies related to the effects of the climate change on the environment, CMIP3 to CMIP6 models have had satisfactory results in various researches (Sharafati and Pezeshki 2020; Shadkam et al. 2016; Vaghefi et al. 2019). The present research has used the CMIP5 model to study the effects of the climate change on runoffs and hydrological drought, and, among the selected models and scenarios, Miroc5 model under the RCP8.5 scenario had the best predictions for the Alvand mountainous basin. Comparing the results of CMIP5 (used in this study) with those of CMIP6 (relatively new) have shown that ACCESS-CM2 and Miroc5 models have good rainfall predictability in, respectively, CMIP6 and CMIP5 (Kamruzzaman et al. 2021). Zamani et al. (2021), too, have shown that CMIP5 performs better than CMIP6 in the fall season, but, in general, CMIP6 predicts the rainfall and temperature more accurately. Many global-scale GCM models have been developed to predict the future climate conditions (Hoegh-Guldberg et al. 2019; Piao et al. 2019). Since uncertainty is central in GCMs, and natural variability and resolution can affect them, downscaling is essential to adapt outputs of GCMs and conditions of the desired area (Zhou et al. 2020); among conventional techniques, random downscaling is the one worth mentioning. The Lars-WG model allows the user to generate daily weather data considering the changes in the variables. GCM results under different scenarios showed that Lars-WG predicted the air temperature better than the rainfall, which is consistent with the results of Doulabian et al. (2021). The very practical
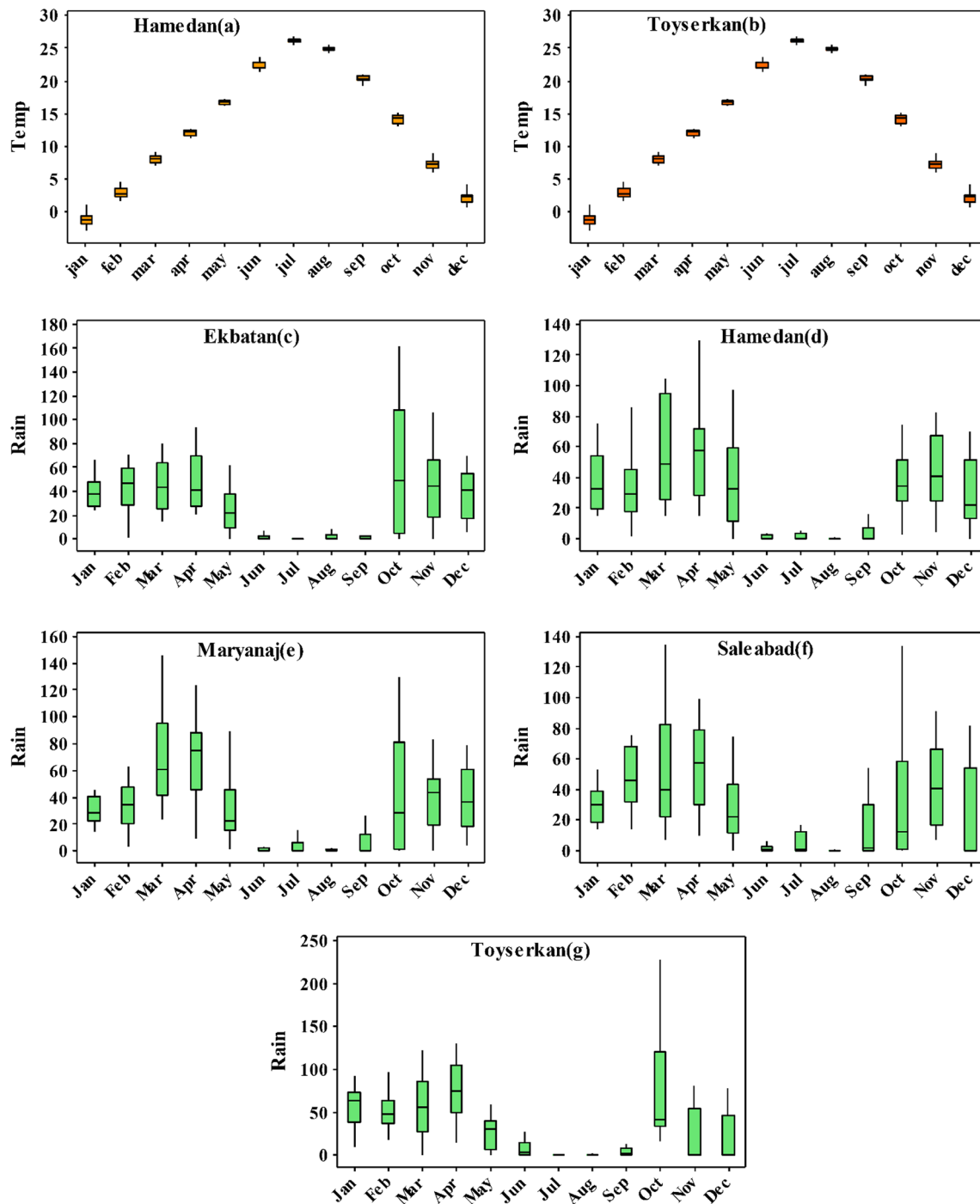
Fig. 8 Future temperature and rainfall boxplots

semi-distributive SWAT model requires future temperature and rainfall to estimate the future river-flow. Analyzing future river-flow characteristics such as the presence of a significant trend/homogeneity or occurrence of hydrological drought conditions is vital to make proper decisions on issues related to the basin assessment/planning systems. The above

model has simulated the studied area well, but has been relatively erroneous in simulating the runoff peak, which is consistent with the results of Sharafati and Pezeshki (2020) and Zakizadeh et al. (2021); however, this weakness does not hinder the study of hydrological drought, which is the primary objective of this research. General results of climate
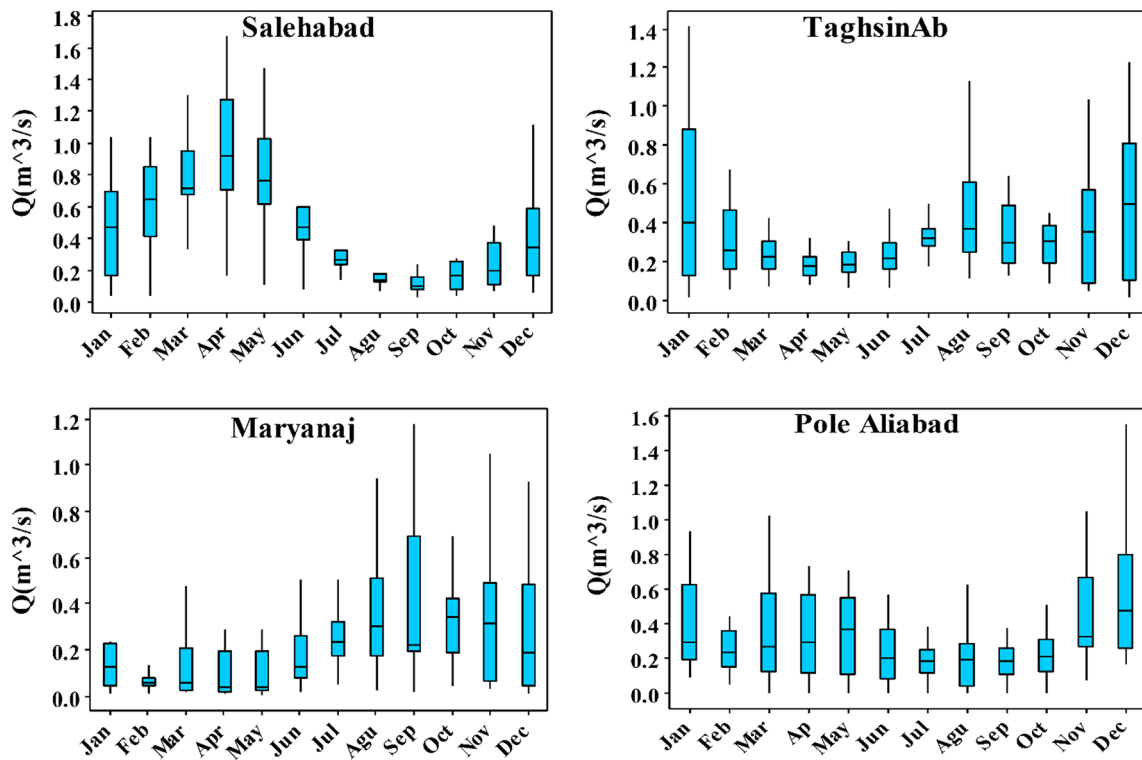
Fig. 9 Future runoff boxplots

Table 9 Percent future runoff variations based on past measurements

	GFDL-CM3 (RCP4.5)	GFDL-CM3 (RCP8.5)	EC_EARTH (RCP4.5)	EC_EARTH (RCP8.5)	Hadgem2_ES (RCP4.5)	Hadgem2_ES (RCP8.5)	Miroc5 (RCP4.5)	Miroc5 (RCP8.5)
SalehAbad	−20.98	−54.44	−51.95	−17.93	−18.58	−66.77	−71.07	−11.65
Maryanaj	−51.39	−85.35	−85.36	−72.72	−72.71	−93.73	−91.37	−2.56
TaghsimAb	−63.90	−85.75	−85.87	−77.39	−77.39	−91.86	−77.39	−12.69
Pole Aliabad	−54.81	−44.79	−44.49	−33.58	−34.49	−50.37	−48.35	−6.55
Average	−47.77	−67.5825	−66.9175	−50.405	−50.7925	−75.6825	−72.045	−8.3625

change studies on runoffs in the region (under the models and scenarios mentioned in this study) have shown that runoffs will decrease significantly during 2020 to 2040 due to reduced rainfalls and increased temperature. These results do not conform to those of Zakizadeh et al.'s (2021) found in

relatively flat Darabad area, Tehran (Iran) that show (under RCP2.6, RCP4.5 and RCP8.5 scenarios with the CanESM2 model) runoffs will increase in the mentioned basin. It seems that the decrease in runoff will be due to reduced snowfalls in the region because the past years' decreasing snowfall trend

Table 10 Percent runoff variations in all seasons and for all periods and scenarios in relation to the past

	Winter		Spring		Summer		Fall	
	RCP4.5 (%)	RCP8.5 (%)	RCP4.5 (%)	RCP8.5 (%)	RCP4.5 (%)	RCP8.5 (%)	RCP4.5 (%)	RCP8.5 (%)
GFDL-CM3								
SalehAbad	−77	−77	−80	−80	38	38	−52	−52
Maryanaj	−94	−95	−94	−96	−76	−83	−89	−91
TaghsimAb	−60	−91	−86	−95	−64	−83	−71	−91
Pole Aliabad	−9	−11	−63	−66	−88	−88	20	17
average	−60	−69	−81	−84	−48	−54	−48	−54
EC_EARTH								
SalehAbad	4	4	−47	−47	181	181	118	118
Maryanaj	−54	−54	−83	−83	−48	−48	−63	−63
TaghsimAb	−60	−60	−86	−86	−64	−64	−71	−71
Pole Aliabad	5	14	−60	−60	−95	−93	141	131
average	31	−26	−24	−69	−69	−7	−6	31
Hadgem2_ES								
SalehAbad	−48	−50	−65	−70	80	80	−19	6
Maryanaj	−82	−81	−90	−91	−68	−68	−86	−83
TaghsimAb	−79	−79	−90	−91	−76	−74	−87	−84
Pole Aliabad	4	−9	−66	−64	−94	−92	66	69
average	−32	−51	−55	−78	−79	−40	−39	−32
Miroc5								
SalehAbad	−31	0	−49	−43	154	239	−2	106
Maryanaj	−15	−22	−65	−85	−16	157	−70	294
TaghsimAb	−27	62	−75	−81	−51	59	−76	133
Pole Aliabad	−11	56	−77	−59	−77	−59	74	123
average	−21	24	−67	−67	3	99	−19	164
Total Average	−17	−40	−31	−74	−75	−23	0	−17

approves it; hence, it can be concluded that snowfalls will decrease during 2020 to 2040 causing runoffs to decrease in dry seasons.

5 Conclusion

The current study used the soil and water assessment tool (SWAT) with SUFI2 algorithm to evaluate the past daily and monthly runoffs, predicted the effects of 4 CMIP5 climate models (Hadgem2_ES, EC_EARTH, GFDL-CM3, Miroc5) and two emission scenarios (RCP4.5 and RCP8.5) on 5 meteorological stations (Ekbatan, SalehAbad, Maryanaj, Pole Aliabad, and TaghsimAb in Alvand mountain basin and studied the effects of climate variations on the monthly flow. According to the results, SWAT simulated the daily and monthly runoffs well and was quite capable in the Alvand mountain basin. The results showed that, the best model for the prediction of temperature and rainfall in the region was the Miroc5 model with the RCP8.5 scenario among the climate change models from Cmip5. According to the results found from the mentioned models and

Table 11 Percent runoff variations in all months for all periods and scenarios in relation

	January		February		March		April		May		June	
	RCP4.5 (%)	RCP8.5 (%)	RCP4.5 (%)	RCP8.5 (%)	RCP4.5 (%)	RCP8.5 (%)	RCP4.5 (%)	RCP8.5 (%)	RCP4.5 (%)	RCP8.5 (%)	RCP4.5 (%)	RCP8.5 (%)
GFDL-CM3												
SalehAbad	−77	−77	−75	−75	−86	−86	−82	−82	−69	−69	9	9
Maryanaj	−93	−94	−94	−95	−94	−95	−95	−96	−94	−96	−84	−89
TaghsimAb	−51	−89	−69	−91	−85	−96	−86	−95	−85	−94	−71	−87
Pole Aliabad	19	13	−45	−48	−34	−40	−73	−75	−73	−72	−98	−98
Average	−51	−62	−71	−77	−75	−79	−84	−87	−80	−83	−61	−66
EC_EARTH												
SalehAbad	13	13	−11	−11	−50	−50	−54	−54	−33	−33	119	119
Maryanaj	−45	−45	−62	−62	−76	−76	−85	−85	−85	−85	−64	−64
TaghsimAb	−51	−51	−69	−69	−85	−85	−86	−86	−85	−85	−71	−71
Pole Aliabad	33	51	−30	−30	−20	−23	−70	−70	−76	−75	−99	−99
Average	−13	−8	−43	−43	−58	−59	−74	−74	−70	−70	−29	−29
Hadgem2_ES												
SalehAbad	−45	−45	−46	−55	−68	−76	−69	−73	−55	−57	43	42
Maryanaj	−78	−76	−79	−81	−86	−89	−91	−92	−91	−91	−78	−78
TaghsimAb	−73	−73	−79	−82	−90	−92	−91	−91	−90	−90	−80	−79
Pole Aliabad	42	18	−32	−43	−33	−32	−74	−72	−79	−76	−99	−99
Average	−39	−44	−59	−65	−69	−72	−81	−82	−79	−79	−54	−54
Miroc5												
SalehAbad	53	10	15	−11	−45	−49	−58	−50	−41	−22	95	162
Maryanaj	2	−19	−7	−75	−35	−73	−70	−88	−75	−88	−42	−29
TaghsimAb	−9	112	−30	−9	−67	−72	−77	−85	−79	−84	−60	−43
Pole Aliabad	−17	64	−24	−17	−57	−45	−78	−67	−91	−58	−99	−38
Average	7	42	−12	−28	−51	−60	−71	−73	−72	−63	−27	13
Total Average	−21		−50		−65		−78		−74		−38	

	July		August		September		October		November		December	
	RCP4.5 (%)	RCP8.5 (%)	RCP4.5 (%)	RCP8.5 (%)	RCP4.5 (%)	RCP8.5 (%)	RCP4.5 (%)	RCP8.5 (%)	RCP4.5 (%)	RCP8.5 (%)	RCP4.5 (%)	RCP8.5 (%)
GFDL-CM3												
SalehAbad	87	87	151	151	266	266	40	40	−81	−81	−82	−82
Maryanaj	−59	−70	−34	−50	−27	−42	−91	−92	−94	−95	−94	−95
TaghsimAb	−48	−75	−59	−80	−68	−83	−76	−91	−70	−95	−55	−94
Pole Aliabad	−53	−50	−100	−100	−89	−90	52	39	40	40	14	17
Average	−18	−27	−11	−20	21	13	−19	−26	−51	−58	−54	−64
EC_EARTH												
SalehAbad	280	280	443	443	789	789	415	415	41	41	25	25
Maryanaj	−12	−12	35	35	41	41	−75	−75	−65	−65	−52	−52
TaghsimAb	−48	−48	−59	−59	−68	−68	−76	−76	−70	−70	−55	−55
Pole Aliabad	−78	−71	−100	−100	−73	−75	245	212	160	158	26	39
Average	36	37	80	80	172	172	127	119	17	16	−14	−11
Hadgem2_ES												
SalehAbad	140	143	228	234	416	431	127	185	−61	−41	−56	−45
Maryanaj	−46	−45	−15	−13	−8	−7	−88	−86	−92	−87	−89	−84
TaghsimAb	−65	−62	−72	−71	−78	−76	−88	−85	−91	−87	−85	−80

Table 11 (continued)

	July		August		September		October		November		December	
	RCP4.5 (%)	RCP8.5 (%)	RCP4.5 (%)	RCP8.5 (%)	RCP4.5 (%)	RCP8.5 (%)	RCP4.5 (%)	RCP8.5 (%)	RCP4.5 (%)	RCP8.5 (%)	RCP4.5 (%)	RCP8.5 (%)
Pole Aliabad	−76	−65	−100	−100	−86	−84	117	129	89	88	18	13
Average	−12	−7	10	13	61	66	17	36	−39	−32	−53	−49
Miroc5												
SalehAbad	244	365	415	563	692	949	113	416	−53	20	7	10
Maryanaj	41	332	117	1729	122	2943	−76	239	−83	91	−43	50
TaghsimAb	−29	145	−44	327	−55	338	−78	97	−84	74	−43	126
Pole Aliabad	−100	29	−100	80	−84	177	113	114	105	110	14	153
Average	39	218	97	675	169	1102	18	217	−29	74	−16	85
Total Average	33		115		222		61		−13		−22	

Fig. 10 SDI series in study stations for the 2003–2017 period
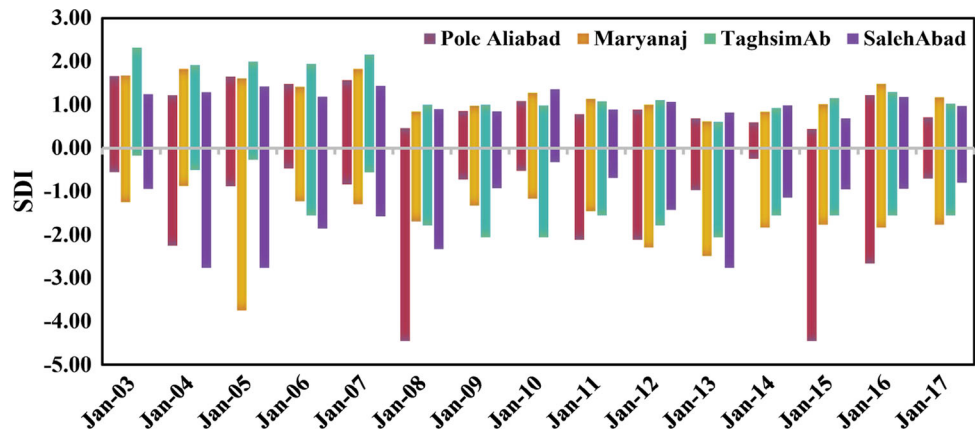
scenarios where GFDL-CM3 model with RCP8.5 scenario predicted the least runoff compared to other models, the 2020–2040 future runoffs will decrease (75.68%) compared to the past and the Alvand mountain basin will face such problems as increased temperature, reduced rainfall and, hence, reduced surface runoff. Also, according to the best model (Miroc5 (RCP8.5)), the amount of runoff will decrease by 8.36. The Mann–Kendall Trend Test results show that the 2020–2040 runoffs will be increasing although the trend is not significant. The SDI calculations also show that the drought severity will increase in future compared to the past which, for the best model (Miroc5 (RCP8.5)) this value was 180%. As the population is growing fast and a large part of the agricultural and
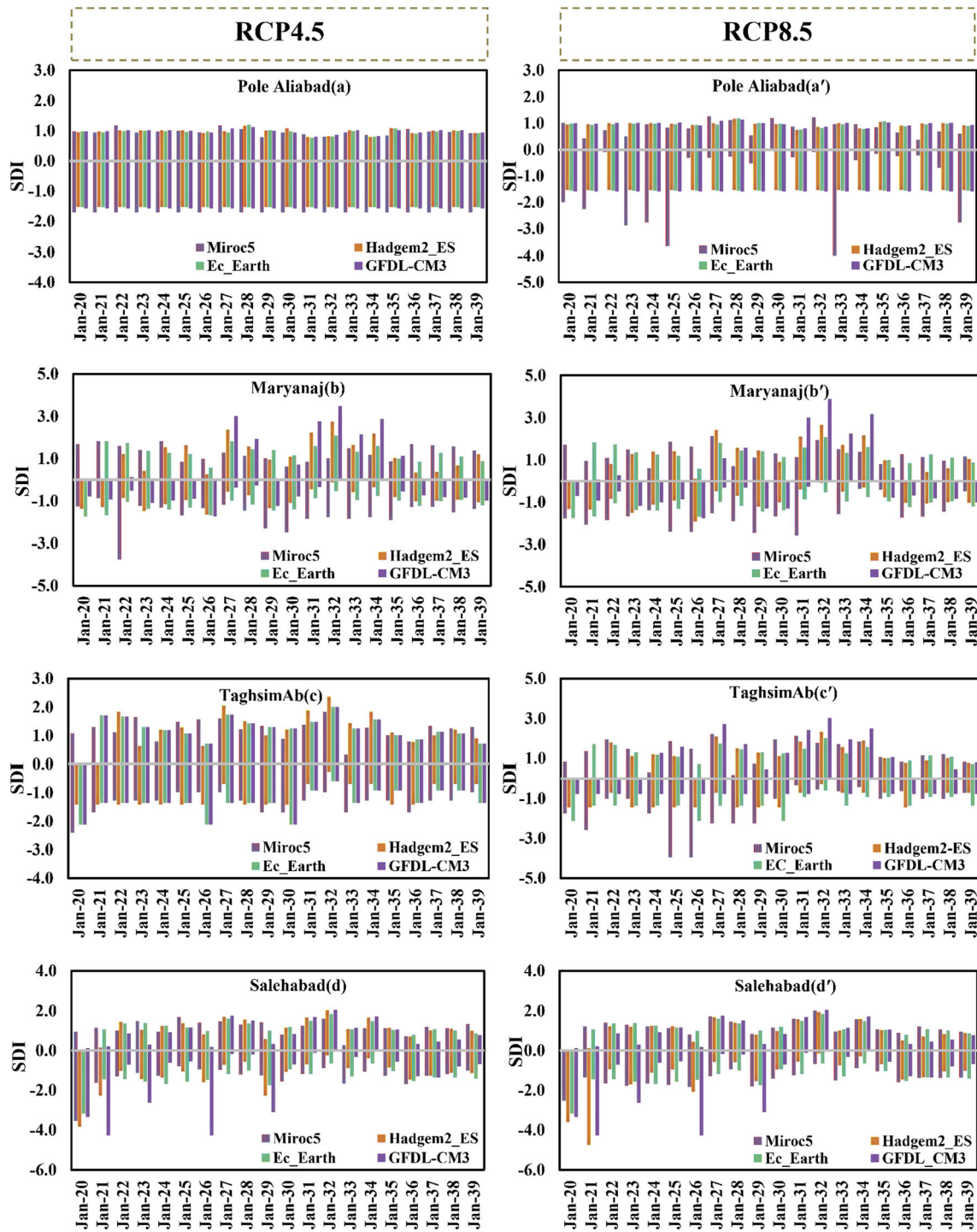
Fig. 11 SDI series in study stations for the 2020–2040 period

domestic water consumption in Hamedan is supplied from

Table 12 Percent future SDI variations compared to the past

	Miroc5 (RCP8.5) (%)	Miroc5 (RCP4.5) (%)	Hadgem2_ES (RCP8.5) (%)	Hadgem2_ES (RCP4.5) (%)	EC-EARTH (RCP8.5) (%)	EC_EARTH (RCP4.5) (%)	GFDL-CM3 (RCP8.5) (%)	GFDL-CM3 (RCP4.5) (%)	Average (%)
Pole Aliabadj									
January	3098	5186	5833	6257	5943	5724	5979	6019	5505
February	11	−266	−155	−220	−170	−175	−153	−159	−161
March	89	−41	−51	−49	−47	−50	−51	−54	−32
April	105	33	25	28	30	29	26	25	38
May	95	61	50	59	54	54	43	44	58
June	152	345	402	421	420	423	383	391	367
July	−6	−471	−297	−304	−311	−311	−235	−243	−272
August	12	−154	−128	−127	−131	−128	−135	−134	−116
September	57	4	3	6	6	1	−10	−7	8
October	89	170	158	159	169	176	146	148	152
November	420	722	615	602	649	646	573	564	599
December	594	712	474	486	496	481	490	470	525
Maryanaj									
January	240	154	5	35	−33	−33	97	165	79
February	271	−93	31	14	32	32	71	101	57
March	167	−21	65	38	38	38	68	82	59
April	155	23	53	34	40	40	58	54	57
May	156	35	43	31	41	41	50	42	55
June	106	−25	−18	−53	−3	−3	−1	−48	−6
July	171	67	80	87	66	66	80	102	90
August	150	53	63	64	52	52	71	79	73
September	144	36	52	52	38	38	68	72	63
October	204	−107	5	−25	−30	−30	38	35	11
November	1803	1444	−1599	−3010	−1196	−1196	−1057	−1414	−778
December	53	131	105	275	11	11	170	243	125
TaghsimAb									
January	207	566	146	176	177	177	−19	177	201
February	118	−175	61	−5	12	12	70	12	13
March	122	10	68	43	49	49	89	49	60
April	133	31	45	34	40	40	59	40	53
May	135	39	38	34	35	35	54	35	51
June	199	−37	−102	−89	−83	−83	−130	−83	−51
July	137	71	103	102	82	82	134	82	99
August	150	33	58	51	40	40	90	40	63
September	123	13	41	42	13	13	69	13	41
October	103	−66	3	−12	−16	−16	28	−16	1
November	106	−308	−94	−201	−27	−27	−109	−27	−86
December	222	88	32	−67	111	111	−111	111	62
SalehAbad									
January	94	−35	82	83	75	75	89	89	69
February	34	−26	40	20	25	25	34	34	23
March	19	9	40	14	18	18	51	51	28
April	3	14	21	6	11	11	25	25	15
May	−22	1	9	−5	1	1	4	4	−1
June	−1017	−585	−571	−710	−563	−563	−788	−788	−698
July	70	49	41	50	44	44	60	60	52

Table 12 (continued)

	Miroc5 (RCP8.5) (%)	Miroc5 (RCP4.5) (%)	Hadgem2_ES (RCP8.5) (%)	Hadgem2_ES (RCP4.5) (%)	EC-EARTH (RCP8.5) (%)	EC_EARTH (RCP4.5) (%)	GFDL-CM3 (RCP8.5) (%)	GFDL-CM3 (RCP4.5) (%)	Average (%)
August	24	23	15	19	16	16	11	11	17
September	17	19	33	27	17	17	40	40	26
October	25	−8	59	37	33	33	68	68	39
November	−813	−1615	−359	−920	−329	−329	−531	−531	−678
December	127	58	72	129	82	82	123	123	100
Average	180	128	119	77	126	121	129	129	126

rivers flowing in the Alvand mountain basin, management plans are quite important in this area and play a key role in providing water resources and solving the future water crises problems.

Declarations

Conflict of interest The authors declare that they have no conflict of interest.

Ethical approval The authors have agreed on the submission of this article and declare it is not currently under any consideration for publication in other journals.

Consent to participate The authors voluntarily agreed to participate in this research study.

Consent for publication The authors approved the publication of this study.

References

Abbaspour KC, Yang J, Maximov I, Siber R, Bogner K, Mieleitner J, Srinivasan R (2007) Modelling hydrology and water quality in the pre-alpine/alpine Thur watershed using SWAT. J Hydrol 333(2–4):413–430. https://doi.org/10.1016/j.jhydrol.2006.09.014

Abbaspour KC, Rouholahnejad E, Vaghefi SRINIVASANB, Srinivasan R, Yang H, Kløve B (2015) A continental-scale hydrology and water quality model for Europe: calibration and uncertainty of a high-resolution large-scale SWAT model. J Hydrol 524:733–752. https://doi.org/10.1016/j.jhydrol.2015.03.027

Abdulai PJ, Chung ES (2019) Uncertainty assessment in drought severities for the Cheongmicheon watershed using multiple GCMs and the reliability ensemble averaging method. SustainBasel 11(16):4283. https://doi.org/10.3390/su11164283

Ahmadi M, Moeini A, Ahmadi H, Motamedvaziri B, Zehtabiyan GR (2019) Comparison of the performance of SWAT, IHACRES and artificial neural networks models in rainfall-runoff simulation (case study: Kan watershed, Iran). Phys Chem Earth Parts a/b/c 111:65–77. https://doi.org/10.1016/j.pce.2019.05.002

Alansi AW, Amin MSM, Abdul Halim G, Shafri HZM, Aimrun W (2009) Validation of SWAT model for stream flow simulation and forecasting in Upper Bernam humid tropical river basin, Malaysia. Hydrol Earth Syst Sci Discus 6(6):7581–7609. https://doi.org/10.5194/hessd-6-7581-2009

Aliyari F, Bailey RT, Tasdighi A, Dozier A, Arabi M, Zeiler K (2019) Coupled SWAT-MODFLOW model for large-scale mixed agro-urban river basins. Environ Model Softw 115:200–210. https://doi.org/10.1016/j.envsoft.2019.02.014

Andrade MA, Mello CRD, Beskow S (2013) Simulação hidrológica em uma bacia hidrográfica representativa dos Latossolos na região Alto Rio Grande, MG. Rev Bras Engenharia Agrícola Ambiental 17:69–76. https://doi.org/10.1590/S1415-43662013000100010

Andrade CW, Montenegro SM, Montenegro AA, Lima JRDS, Srinivasan R, Jones CA (2021) Climate change impact assessment on water resources under RCP scenarios: a case study in Mundaú River Basin, Northeastern Brazil. Int J Climatol 41:E1045–E1061. https://doi.org/10.1002/joc.6751

Arnold JG, Allen PM, Bernhardt G (1993) A comprehensive surface-groundwater flow model. J Hydrol 142(1–4):47–69. https://doi.org/10.1016/0022-1694(93)90004-S

Arnold JG, Srinivasan R, Muttiah RS, Williams JR (1998) Large area hydrologic modeling and assessment part I: model development 1. J Am Water Resour Assoc 34(1):73–89. https://doi.org/10.1111/j.1752-1688.1998.tb05961.x

Arnold J (1994) SWAT-soil and water assessment tool

Ashofteh PS, Haddad OB, Loáiciga HA (2015a) Evaluation of climatic-change impacts on multiobjective reservoir operation with multiobjective genetic programming. J Water Resour Plan Manag 141(11):04015030. https://doi.org/10.1061/(ASCE)WR.1943-5452.0000540

Ashofteh PS, Haddad OB, Marino MA (2015b) Risk analysis of water demand for agricultural crops under climate change. J Hydrol Eng 20(4):04014060. https://doi.org/10.1061/(ASCE)HE.1943-5584.0001053

Ashofteh PS, Bozorg-Haddad O, Loáiciga HA (2017) Impacts of climate change on the conflict between water resources and agricultural water use. J Irrig Drain Eng 143(4):02516002. https://doi.org/10.1061/(ASCE)IR.1943-4774.0001143

Azadi F, Ashofteh PS, Loáiciga HA (2019) Reservoir water-quality projections under climate-change conditions. Water Resour Manag 33(1):401–421. https://doi.org/10.1061/%28ASCE%29IR.1943-4774.0001105

Babaeian F, Delavar M, Morid S, Srinivasan R (2021) Robust climate change adaptation pathways in agricultural water management. Agric Water Manag 252:106904. https://doi.org/10.1016/j.agwat.2021.106904

Bhatta B, Shrestha S, Shrestha PK, Talchabhadel R (2019) Evaluation and application of a SWAT model to assess the climate change

impact on the hydrology of the Himalayan River Basin. CATENA 181:104082. https://doi.org/10.1016/j.catena.2019.104082

Blainski É, Acosta E, Nogueira PCDP (2017) Calibração e validação do modelo SWAT para simulação hidrológica em uma bacia hidrográfica do litoral norte catarinense. Rev Ambiente Água 12:226–237. https://doi.org/10.4136/ambi-agua.1951

Borji M, Malekian A, Salajegheh A, Ghadimi M (2016) Multi-timescale analysis of hydrological drought forecasting using support vector regression (SVR) and artificial neural networks (ANN). Arab J Geosci 9(19):725. https://doi.org/10.1007/s12517-016-2750-x

Chang HS, Su Q (2021) Exploring the coupling relationship of stormwater runoff distribution in watershed from the perspective of fairness. Urban Clim 36:100792. https://doi.org/10.1016/j.uclim.2021.100792

Change IC (2013) The physical science basis. Contribution of working group I to the fifth assessment report of the intergovernmental panel on climate change, 1535

Chen Y, Xu CY, Chen X, Xu Y, Yin Y, Gao L, Liu M (2019) Uncertainty in simulation of land-use change impacts on catchment runoff with multi-timescales based on the comparison of the HSPF and SWAT models. J Hydrol 573:486–500. https://doi.org/10.1016/j.jhydrol.2019.03.091

Chow TJ, Patterson CC (1959) Lead isotopes in manganese nodules. Geochim Cosmochim Acta 17(1–2):21–31. https://doi.org/10.1016/0016-7037(59)90075-4

Chu ML, Knouft JH, Ghulam A, Guzman JA, Pan Z (2013) Impacts of urbanization on river flow frequency: a controlled experimental modeling-based evaluation approach. J Hydrol 495:1–12. https://doi.org/10.1016/j.jhydrol.2013.04.051

Cibin R, Sudheer KP, Chaubey I (2010) Sensitivity and identifiability of stream flow generation parameters of the SWAT model. Hydrol Process Int J 24(9):1133–1148. https://doi.org/10.1002/hyp.7568

Cornelissen T, Diekkrüger B, Giertz S (2013) A comparison of hydrological models for assessing the impact of land use and climate change on discharge in a tropical catchment. J Hydrol 498:221–236. https://doi.org/10.1016/j.jhydrol.2013.06.016

de Andrade CW, Montenegro SM, Montenegro AA, Lima JRDS, Srinivasan R, Jones CA (2019) Soil moisture and discharge modeling in a representative watershed in northeastern Brazil using SWAT. Ecohydrol Hydrobiol 19(2):238–251. https://doi.org/10.1016/j.ecohyd.2018.09.002

dos Santos JYG, Montenegro SMGL, da Silva RM, Santos CAG, Quinn NW, Dantas APX, Neto AR (2021) Modeling the impacts of future LULC and climate change on runoff and sediment yield in a strategic basin in the Caatinga/Atlantic forest ecotone of Brazil. CATENA 203:105308. https://doi.org/10.1016/j.catena.2021.105308

Doulabian S, Golian S, Toosi AS, Murphy C (2021) Evaluating the effects of climate change on precipitation and temperature for Iran using RCP scenarios. J Water Clim Change 12(1):166–184. https://doi.org/10.2166/wcc.2020.114

Ercan MB, Maghami I, Bowes BD, Morsy MM, Goodall JL (2020) Estimating potential climate change effects on the upper neuse watershed water balance using the SWAT model. J Am Water Resour Assoc 56(1):53–67. https://doi.org/10.1111/1752-1688.12813

Escanilla-Minchel R, Alcayaga H, Soto-Alvarez M, Kinnard C, Urrutia R (2020) Evaluation of the impact of climate change on runoff generation in an andean glacier watershed. Water 12(12):3547. https://doi.org/10.3390/w12123547

Fereidoon M, Koch M, Brocca L (2019) Predicting rainfall and runoff through satellite soil moisture data and SWAT modelling for a poorly gauged basin in Iran. Water 11(3):594. https://doi.org/10.3390/w11030594

Gebremariam SY, Martin JF, DeMarchi C, Bosch NS, Confesor R, Ludsin SA (2014) A comprehensive approach to evaluating watershed models for predicting river flow regimes critical to downstream ecosystem services. Environ Model Softw 61:121–134. https://doi.org/10.1016/j.envsoft.2014.07.004

Goyal MK, Panchariya VK, Sharma A, Singh V (2018) Comparative assessment of SWAT model performance in two distinct catchments under various DEM scenarios of varying resolution, sources and resampling methods. Water Resour Manag 32(2):805–825. https://doi.org/10.1016/j.jhydrol.2015.03.027

Hammouri N, Adamowski J, Freiwan M, Prasher S (2017) Climate change impacts on surface water resources in arid and semi-arid regions: a case study in northern Jordan. Acta Geod Geoph 52(1):141–156. https://doi.org/10.1007/s40328-016-0163-7

Hoegh-Guldberg O, Jacob D, Taylor M, Guillén Bolaños T, Bindi M, Brown S, Zhou G (2019) The human imperative of stabilizing global climate change at 1.5 C. Science 365(6459):6974. https://doi.org/10.1126/science.aaw6974

Kaffas K, Hrissanthou V, Sevastas S (2018) Modeling hydromorphological processes in a mountainous basin using a composite mathematical model and ArcSWAT. CATENA 162:108–129. https://doi.org/10.1016/j.catena.2017.11.017

Kamali B, Kouchi DH, Yang H, Abbaspour KC (2017) Multilevel drought hazard assessment under climate change scenarios in semi-arid regions-a case study of the karkheh river basin in Iran. Water-SUI. https://doi.org/10.3390/w9040241

Kamruzzaman M, Shahid S, Islam ARM, Hwang S, Cho J, Zaman M, Hossain M (2021) Comparison of CMIP6 and CMIP5 model performance in simulating historical precipitation and temperature in Bangladesh: a preliminary study. Theoret Appl Climatol 145(3):1385–1406. https://doi.org/10.1007/s00704-021-03691-0

Kendall MG (1975) Rank correlation methods. 2nd impression. Charles Griffin and Company Ltd. London and High Wycombe

Khazaei M, Mirzaei MR (2013) Comparison of monthly discharge prediction efficiency using artificial neural network methods and time series. Watershed Eng Manag 5(2):74–84. https://doi.org/10.22092/ijwmse.2013.101803

Kiprotich P, Wei X, Zhang Z, Ngigi T, Qiu F, Wang L (2021) Assessing the impact of land use and climate change on surface runoff response using gridded observations and SWAT+. Hydrology 8(1):48. https://doi.org/10.3390/hydrology8010048

Li X, Xie SP, Gille ST, Yoo C (2016) Atlantic-induced pan-tropical climate change over the past three decades. Nat Clim Chang 6(3):275–279. https://doi.org/10.1038/nclimate2840

Li Z, Li Q, Wang J, Feng Y, Shao Q (2021) Corrigendum to" Impacts of projected climate change on runoff in upper reach of Heihe River basin using climate elasticity method and GCMs" [Sci. Total Environ., 716 (2020) 137072]. Sci Total Environ 766:142628. https://doi.org/10.1016/j.scitotenv.2020.137072

Lian Y, Sun M, Wang J, Luan Q, Jiao M, Zhao X, Gao X (2021) Quantitative impacts of climate change and human activities on the runoff evolution process in the Yanhe River Basin. Phys Chem Earth Parts a/b/c 122:102998. https://doi.org/10.1016/j.pce.2021.102998

Lin K, Lv F, Chen L, Singh VP, Zhang Q, Chen X (2014) Xinanjiang model combined with Curve Number to simulate the effect of land use change on environmental flow. J Hydrol 519:3142–3152. https://doi.org/10.1016/j.jhydrol.2014.10.049

Liu Z, Merwade V (2018) Accounting for model structure, parameter and input forcing uncertainty in flood inundation modeling using Bayesian model averaging. J Hydrol 565:138–149. https://doi.org/10.1016/j.jhydrol.2018.08.009

Liu Z, Herman JD, Huang G, Kadir T, Dahlke HE (2021) Identifying climate change impacts on surface water supply in the southern Central Valley, California. Sci Total Environ 759:143429. https://doi.org/10.1016/j.scitotenv.2020.143429

Malik A, Kumar A, Singh RP (2019) Application of heuristic approaches for prediction of hydrological drought using multi-scalar streamflow drought index. Water Resour Manag 33(11):3985–4006. https://doi.org/10.1007/s11269-019-02350-4

Mann HB (1945) Nonparametric tests against trend. Econometrica 13:245–259. https://doi.org/10.2307/1907187

McKee TB, Doesken NJ, Kleist J (1993) The relationship of drought frequency and duration to time scales. In: Proceedings of the 8th conference on applied climatology, vol 17, no 22, pp 179–183

Mishra AK, Singh VP (2010) A review of drought concepts. J Hydrol 391(1–2):202–216

Moriasi DN, Arnold JG, Van Liew MW, Bingner RL, Harmel RD, Veith TL (2007) Model evaluation guidelines for systematic quantification of accuracy in watershed simulations. Trans ASABE 50(3):885–900. https://doi.org/10.13031/2013.23153

Myronidis D, Ioannou K, Fotakis D, Dörflinger G (2018) Streamflow and hydrological drought trend analysis and forecasting in Cyprus. Water Resour Manag 32(5):1759–1776. https://doi.org/10.1007/s11269-018-1902-z

Nalbantis I, Tsakiris G (2009) Assessment of hydrological drought revisited. Water Resour Manag 23(5):881–897. https://doi.org/10.1007/s11269-008-9305-1

Neitsch SL, Arnold JG, Kiniry JR, Williams JR (2011) Soil and water assessment tool theoretical documentation version 2009. Texas Water Resources Institute

Pachauri RK, Allen MR, Barros VR, Broome J, Cramer W, Christ R, van Ypserle JP (2014) Climate change 2014: synthesis report. Contribution of Working Groups I, II and III to the fifth assessment report of the Intergovernmental Panel on Climate Change. IPCC, p 151

Pereira DDR, Martinez MA, Almeida AQD, Pruski FF, Silva DDD, Zonta JH (2014) Hydrological simulation using SWAT model in headwater basin in Southeast Brazil. Engenharia Agrícola 34:789–799. https://doi.org/10.1590/S0100-69162014000400018

Piao S, Liu Q, Chen A, Janssens IA, Fu Y, Dai J, Zhu X (2019) Plant phenology and global climate change: current progresses and challenges. Glob Change Biol 25(6):1922–1940. https://doi.org/10.1111/gcb.14619

Rajib MA, Merwade V, Yu Z (2016) Multi-objective calibration of a hydrologic model using spatially distributed remotely sensed/in-situ soil moisture. J Hydrol 536:192–207. https://doi.org/10.1016/j.jhydrol.2016.02.037

Ridwansyah I, Yulianti M, Onodera SI, Shimizu Y, Wibowo H, Fakhrudin M (2020) The impact of land use and climate change on surface runoff and groundwater in Cimanuk watershed, Indonesia. Limnology 21(3):487–498. https://doi.org/10.1007/s10201-020-00629-9

Salimi H, Asadi E, Darbandi S (2021) Meteorological and hydrological drought monitoring using several drought indices. Appl Water Sci 11(2):11. https://doi.org/10.1007/s13201-020-01345-6

Semiromi MT, Koch M (2019) Analysis of spatio-temporal variability of surface–groundwater interactions in the Gharehsoo river basin, Iran, using a coupled SWAT-MODFLOW model. Environ Earth Sci 78(6):1–21. https://doi.org/10.1007/s12665-019-8206-3

Sen PK (1968) Estimates of the regression coefficient based on Kendall's tau. J Am Stat Assoc 63(324):1379–1389

Shadkam S, Ludwig F, van Oel P, Kirmit Ç, Kabat P (2016) Impacts of climate change and water resources development on the declining inflow into Iran's Urmia Lake. J Great Lakes Res 42(5):942–952. https://doi.org/10.1016/j.jglr.2016.07.033

Shaigan M, Mehran, Alimohammadi, Abbasrouhani, Hamed (2011) Hydrological modeling of Taleghan basin in GIS environment using SWAT model. Iran Remote Sens GIS 3(2). (in Persian)

Sharafati A, Pezeshki E (2020) A strategy to assess the uncertainty of a climate change impact on extreme hydrological events in the semi-arid Dehbar catchment in Iran. Theoret Appl Climatol 139(1):389–402. https://doi.org/10.1007/s00704-019-02979-6

Sharifi A, Yen H, Boomer KM, Kalin L, Li X, Weller DE (2017) Using multiple watershed models to assess the water quality impacts of alternate land development scenarios for a small community. CATENA 150:87–99. https://doi.org/10.1016/j.catena.2016.11.009

Su X, Li X, Niu Z, Liang X (2021) A new complexity-based three-stage method to comprehensively quantify positive/negative contribution rates of climate change and human activities to changes in runoff in the upper Yellow River. J Clean Prod 287:125017. https://doi.org/10.1016/j.jclepro.2020.125017

Tabari H, Nikbakht J, Talaee PH (2013) Hydrological drought assessment in Northwestern Iran based on streamflow drought index (SDI). Water Resour Manag 27(1):137–151. https://doi.org/10.1007/s11269-012-0173-3

Tan ML, Yusop Z, Chua VP, Chan NW (2017) Climate change impacts under CMIP5 RCP scenarios on water resources of the Kelantan River Basin, Malaysia. Atmos Res 189:1–10. https://doi.org/10.1016/j.atmosres.2017.01.008

Theil H (1950) A rank-invariant method of linear and polynomial regression analysis. Indag Math 12(85):173

Vaghefi SA, Keykhai M, Jahanbakhshi F, Sheikholeslami J, Ahmadi A, Yang H, Abbaspour KC (2019) The future of extreme climate in Iran. Sci Rep 9(1):1–11. https://doi.org/10.1038/s41598-018-38071-8

Wodaje GG, Asfaw ZE, Denboba MA (2021) Impacts and uncertainties of climate change on stream flow of the Bilate River (Ethiopia), using a CMIP5 general circulation models ensemble. Int J Water Resour Environ Eng 13(1):64–75. https://doi.org/10.5897/IJWREE2020.0973

Xue C, Chen B, Wu H (2014) Parameter uncertainty analysis of surface flow and sediment yield in the Huolin Basin, China. J Hydrol Eng 19(6):1224–1236. https://doi.org/10.1061/(ASCE)HE.1943-5584.0000909

Xue D, Zhou J, Zhao X, Liu C, Wei W, Yang X, Zhao Y (2021) Impacts of climate change and human activities on runoff change in a typical arid watershed, NW China. Ecol Indic 121:107013. https://doi.org/10.1016/j.ecolind.2020.107013

Zakizadeh HR, Ahmadi H, Zehtabiyan GR, Moeini A, Moghaddamnia A (2021) Impact of climate change on surface runoff: a case study of the Darabad River, northeast of Iran. J Water Clim Change 12(1):82–100. https://doi.org/10.2166/wcc.2020.089

Zettam A, Taleb A, Sauvage S, Boithias L, Belaidi N, Sánchez-Pérez JM (2017) Modelling hydrology and sediment transport in a semi-arid and anthropized catchment using the SWAT model: the case of the Tafna river (northwest Algeria). Water 9(3):216. https://doi.org/10.3390/w9030216

Zhang D, Chen X, Yao H, Lin B (2015) Improved calibration scheme of SWAT by separating wet and dry seasons. Ecol Model 301:54–61. https://doi.org/10.1016/j.ecolmodel.2015.01.018

Zhou L, Meng Y, Vaghefi SA, Marras PA, Sui C, Lu C, Abbaspour KC (2020) Uncertainty-based metal budget assessment at the watershed scale: implications for environmental management practices. J Hydrol 584:124699. https://doi.org/10.1016/j.jhydrol.2020.124699